Water Research 276 (2025) 123238

Contents lists available at ScienceDirect

Water Research

journal homepage: www.elsevier.com/locate/watres

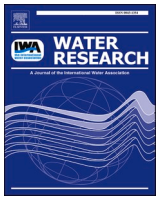

Accounting for model parameter uncertainty provides more robust projections of dissolved organic carbon dynamics to aid drinking water management

Ricardo Paíz [a,*], Donald C. Pierson [b], Klara Lindqvist [c,d], Pamela S. Naden [e], Elvira de Eyto [f], Mary Dillane [f], Valerie McCarthy [g], Suzanne Linnane [a], Eleanor Jennings [a]

[a] Centre for Freshwater and Environmental Studies, Dundalk Institute of Technology, A91 K584 Dundalk, Co. Louth, Ireland
[b] Department of Ecology and Genetics – Limnology, Uppsala University, 752 36 Uppsala, Sweden
[c] Department of Earth Sciences, Uppsala University, 752 36 Uppsala, Sweden
[d] Swedish Meteorological and Hydrological Institute, 601 76 Norrköping, Sweden
[e] UK Centre for Ecology and Hydrology, Crowmarsh Gifford, Wallingford, Oxfordshire OX10 8BB, UK
[f] Fisheries & Ecosystem Advisory Services, Marine Institute, F28 PF65 Newport, Co. Mayo, Ireland
[g] School of History and Geography, Dublin City University, D09 YT18 9, Dublin, Ireland

ARTICLE INFO

Keywords:
Hydrological modelling
Water quality modelling
DOC
Climate change
Uncertainty analysis
GLWF

ABSTRACT

Changes in climate and human behaviour impact catchment hydrology and the export of nutrients including dissolved organic carbon (DOC), with consequences for drinking water supply. In this study, we projected future river discharge and DOC dynamics under three Shared Socioeconomic Pathways (i.e., different futures of climatic conditions, socio-economic development and adaptation to climate change) and quantified change relative to a baseline for two contrasting catchments: one in Sweden and one in Ireland. For this, we used the Generalised Watershed Loading Functions Model (GWLF) with an integrated DOC module (GWLF-DOC) and drove it with data from an ensemble of global climate models, taking into account variability derived from multiple model parameter sets. We assessed the relative contribution of each of these two factors (climate input data and model parameterisation) to the total uncertainty in predictions. Projections for river discharge differed between the two sites in magnitude, variability and direction of change depending on the future scenario and time period. In contrast, DOC was always projected to show increases in concentration throughout the annual cycle and over time, with the highest levels by the end of the century, for scenarios with greater warming and low mitigation efforts. Future climate data provided the dominant source of uncertainty in all of our projections. However, the DOC model parameters, which respond to temperature and soil moisture conditions, became more influential in scenarios of higher climatic variability. Our approach highlights the benefits of incorporating often ignored parameter uncertainty in climate change impact assessments for both interpreting outputs and communicating results to water managers.

1. Introduction

Terrestrially sourced dissolved organic matter (DOM) entering freshwaters has many impacts on aquatic ecology (Rodríguez-Cardona et al., 2022) and on water use and supply (Johnes et al., 2023). High concentrations are associated with water browning (Kritzberg et al., 2020), a condition that affects both ecosystem function (Evans et al., 2005) and drinking water quality (Riyadh and Peleato, 2024). Concentrations of DOM (operationally quantified using dissolved organic carbon (DOC)) must be reduced during drinking water treatment prior to any chlorination (Köhler et al., 2016; Piai et al., 2024), as it is a precursor to the formation of disinfection by-products (DBPs) (Srivastav et al., 2020; Franklin et al., 2021). The presence of DBPs in drinking water, although unintended, remains a critical safety issue due to the adverse effects of DBPs such as trihalomethanes (THMs) on human health (Diana et al., 2019; Kumari and Gupta, 2022). The formation of these contaminants has raised concern in many regions (Villanueva et al., 2023), especially those where DOC drains from terrestrial soil

* Corresponding author.
E-mail address: ricardo.marroquinpaiz@dkit.ie (R. Paíz).

https://doi.org/10.1016/j.watres.2025.123238
Received 2 December 2024; Received in revised form 28 January 2025; Accepted 31 January 2025
Available online 1 February 2025

stores that are rich in organic carbon (e.g., from peatlands and other organic soils) (Xu et al., 2020; Fenner et al., 2021).

The production and transport of DOC in catchments result from interactions between landscape, land use and climate, including atmospheric deposition factors (Jennings et al., 2010; Adler et al., 2021). Temperature, water availability and acid deposition (e.g., sulphur deposition) influence physicochemical and biological mechanisms that regulate soil decomposition and hence DOC production, while hydrological processes control its transport (Evans et al., 2006; Clark et al., 2009; Wit et al., 2021). All of these factors have been reported as drivers of long-term DOC increases in recent decades across the northern hemisphere, although the importance of any factor can vary from site to site (Evans et al., 2005; de Wit et al., 2007; Oulehle and Hruška, 2009; SanClements et al., 2012; Anderson et al., 2023). However, with acid deposition gradually levelling off (Garmo et al., 2014; Wit et al., 2021), the interactions between the other climatic factors and catchment hydrology will likely be more relevant in future DOC dynamics (Clark et al., 2010; Anderson et al., 2023; Wu and Yao, 2024).

Increasingly variable temperature and precipitation patterns, including those related to global warming (Wang et al., 2017; van der Wiel and Bintanja, 2021), can induce important changes in the magnitude and seasonality of DOC export. For instance, dry periods (e.g., hotter, drier summers), wet periods (e.g., wetter winters), prolonged dry conditions, drought-rewetting cycles, lower water tables, and flooding, can all lead to higher variability in catchment DOC concentrations and fluxes (Blaurock et al., 2021; Dong et al., 2021; Wu and Yao, 2022; Wu et al., 2023a, 2023b) that can, in turn, result in higher DBP levels following treatment (Warner and Saros, 2019; Fenner et al., 2021). Increased variability in source water DOC levels can also make water treatment more difficult to manage (Köhler et al., 2016; Piai et al., 2024). It is important, therefore, to quantify the response of both catchment hydrology and DOC dynamics to future climatic conditions. By determining this, drinking water managers may better anticipate future DOC levels, assess risk for supplies, and prepare basin and/or treatment scale mitigation actions accordingly (Ritson et al., 2014; Xu et al., 2020; Klante et al., 2022).

Catchment modelling exercises allow us to quantify change between past and future water quantity and quality, including DOC concentrations and flux. However, all modelling is associated with differing degrees of uncertainty, that are related to a range of sources (Hattermann et al., 2018; Her et al., 2019a). While uncertainty related to projecting future climate (by using ensembles of global climate models [GCMs]) and to human behaviour (by use of multiple scenarios for population behaviour) are now generally incorporated into climate change impact assessments (Kundzewicz et al., 2018; Schürz et al., 2019), other sources are generally not. These include variability related to climate bias correction methods, model structure and model parameterisation i.e., the model state variables, governing equations and parameter selection. Model parameterisation, in particular, can be a complex source of uncertainty since differing sets of parameters can produce equally good simulations of key model variables during calibration (i.e., model parameter equifinality) (Beven and Binley, 1992, 2014), but produce differing results in future scenarios. This uncertainty has been quantified in some studies of changes in DOC dynamics (e.g., O'Driscoll et al., 2018a; Xu et al., 2020), but to date, has not been incorporated into climate change impact simulations. Moreover, the relative contribution of both GCM uncertainty and parameter uncertainty to these future projections has not been explored. Accounting for such uncertainty in future projections will produce more robust outputs (Her et al., 2019a; Marshall et al., 2021), and therefore provide more appropriate information to assist decision making at a catchment management level (Teweldebrhan et al., 2018; Cui et al., 2021).

In this study, we used a previously described DOC model (Naden et al., 2010) that is coupled with the Generalised Watershed Loading Functions Model (GWLF) (Schneiderman et al., 2010) to calibrate and simulate future discharge, DOC concentration and DOC flux under climate change scenarios in one Irish and one Swedish catchment. These sites were selected as they are contrasting in size, climate and hydrology, with high organic soils, and represent systems in countries where drinking water is affected by increases in DOC (O'Driscoll et al., 2018b; Kritzberg et al., 2020), leading to issues in treatment and supply. After years of continuous THM exceedances in several supplies, Ireland has recently been ruled against by the Court of Justice of the European Union (25 January 2024; Case C-481/22) for failure to fulfil obligations on the quality of water intended for human consumption. Similarly, the formation of DBPs has been a persistent problem in Sweden, affecting many drinking water schemes (Kritzberg et al., 2020) including the supply to its capital Stockholm (Köhler et al., 2016).

Within this context, we aimed to: (1) quantify the future change in catchment discharge, DOC concentration and DOC flux between a historical baseline and three future scenarios; (2) determine the periods in the annual cycle when any future changes will be most relevant; and (3) quantify the relative contribution from future climate conditions and model parametrisation to the total uncertainty in these predictions. We capture and summarise the modelling outputs in a way that would be usable by catchment and source water managers. Lastly, we discuss how these results could assist the drinking water sector.

2. Materials and methods

2.1. Study sites

The Glenamong and Vattholma catchments are located in western Ireland (53° 57′ N, 9° 35′ W) and southeastern Sweden (60° 10′ N, 17° 50′ E), respectively (Fig. 1). Both catchments export relatively large quantities of carbon from terrestrial stores to downstream lakes (Ryder et al., 2014; Doyle et al., 2021; Lindqvist, 2022), reflecting their peatland and forest dominated land covers (Coordination of Information on the Environment—CORINE—classification) (Büttner et al., 2017) (Table 1). The Glenamong River is one of the two main inflows to Lough Feeagh and Vattholma flows into Lake Mälaren, the drinking water source for two million people, including the city of Stockholm. While the Glenamong and Feeagh are not used as a source of potable water, they are intensively monitored sites that are representative of similar rivers and small lakes used as drinking water supplies in the region.

The study sites have contrasting characteristics. The Glenamong is small (18 km^2) and unpopulated, characterised by a relatively high variability in daily river discharge due to high precipitation levels and a steep landscape (Doyle et al., 2019; Jennings et al., 2020). Vattholma, in contrast, hosts several communities in a much larger area (261 km^2) and features more gradual variations in daily discharge reflecting a much flatter terrain, longer river network, lower precipitation levels and cooler air temperatures. Vattholma is also drier than Glenamong, only registering measurable rainfall on 37 % of days within a calendar year versus 84 % at the Irish site. While the average DOC concentration recorded at Vattholma is over twice that of the Glenamong, the annual DOC flux on an areal basis is four times lower for the Swedish site due to its much larger basin area (Fig. 1; Table 1).

2.1.1. Data availability

Observed climate data for Vattholma were obtained from the European Climate Assessment & Dataset E-OBS repository (0.1°grid, www.ecad.eu). Daily discharge data at the river outlet (1980–2022) were obtained from the Swedish Meteorological and Hydrological Institute monitoring services (www.smhi.se). Monthly measurements of total organic carbon (TOC) (mg TOC L^{-1}) concentrations at the outlet (1991–2022) were obtained from the Swedish Agricultural University monitoring services (www.slu.se) and were used as a direct proxy for DOC (mg DOC L^{-1}) in line with previous studies for this and other Swedish catchments (e.g., Ledesma et al., 2012; Lindqvist, 2022); TOC = 0.95 DOC + 1.4, $r^2 = 0.93$, $n = 47$. In Glenamong, climate observations from local meteorological stations and daily river discharge data (2013

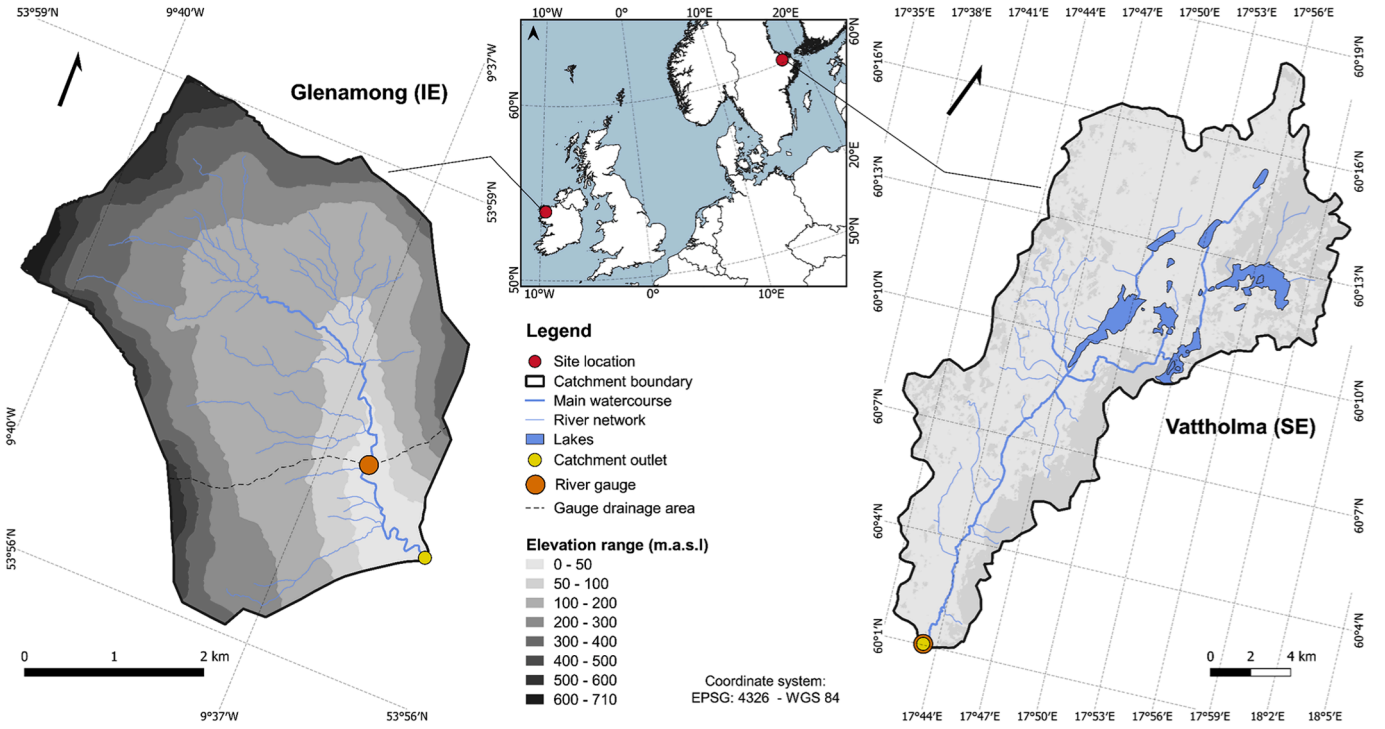

Fig. 1. Location of the study catchments including river network and topographic elevation.

Table 1
Main characteristics of the study catchments. Units for altitude are meters above sea level (m.a.s.l.).

Catchment	Glenamong (IE)	Vattholma (SE)
Area (km^2)	18	261
Altitude range (m.a.s.l.)	8–710	5–83
Main soil type	Blanket peat	Silty clay
Land cover		
Peatland	69 %	5 %
Agriculture	0 %	17 %
Grassland	4 %	15 %
Urban	0 %	2 %
Forest	26 %	58 %
Watercourse	1 %	3 %
Climate and hydrology	*2013–2023*	*1980–2022*
Mean air temperature (°C)	10.8	6.0
Annual precipitation range (mm yr^{-1})	1660–2570	460–875
Mean annual precipitation (mm yr^{-1})	2050	610
Main watercourse length (km)	4.8	39.1
Median river discharge (m^3 s^{-1})	0.4	1.1
Mean river discharge (m^3 s^{-1})	0.8	1.7
Q5 river discharge (m^3 s^{-1})	2.8	5.3
DOC	*2016–2023*	*1992–2022*
DOC concentration range (mg L^{-1})	2.8–18.0	8.2–36.9
Mean DOC concentration (mg L^{-1})	8.7	19.6
Mean annual DOC flux (tC km^{-2} yr^{-1})	16.2	4.0
Mean monthly DOC flux (tC km^{-2} month^{-1})	1.4	0.3

to 2023) were obtained from the Marine Institute monitoring services (https://www.marine.ie). Weekly water colour measurements (expressed as mg PtCo L^{-1}) were also available (2016–2023), based on absorption measurements performed with a HACH Dr 2000 spectrophotometer at 455 nm (wavelength accuracy of ±2 nm) on water filtered through Whatman GF/C filters (1.2 µm pore size). These were used as a proxy for DOC (Doyle et al., 2019), converted via a linear regression relationship with DOC laboratory measurements (samples filtered through 0.45 µm pore size); DOC = 0.067 water colour + 2.69, r^2 = 0.88, n = 551. Observed daily DOC fluxes (kg C km^{-2} day^{-1}) for both sites were computed as the product of DOC concentrations and mean daily measured discharge and normalised to the watershed area.

2.2. The model

The Generalised Watershed Loading Functions Model (GWLF) is a lumped parameter hydrological and water quality model introduced by Haith and Shoemaker (1987). It simulates water balance, water partition among the different flow pathways, sediment loading and nutrient export in a daily time step. The model input requirements include daily time series of precipitation and air temperature as well as land cover, land use, and soil characterisation. In this study, we used the GLWF version developed by the New York City Department of Environmental Protection (NYC DEP) (Schneiderman et al., 2002) that was further developed (Naden et al., 2010; Schneiderman et al., 2010) to include a process-based module for DOC. This model has been previously applied to several catchments to quantify changes in DOC export, including in the Lough Feeagh and Mälaren catchments (Naden et al., 2010; Lindqvist, 2022). Three changes were made to the model configuration in the current study, with the aim of improving DOC simulation capacity and better reflect DOC dynamics. These changes did not increase model complexity and do not require additional input data. Below, we describe key features of the base model and the changes we have implemented.

2.2.1. Hydrology module

GWLF simulates discharge from both surface runoff and from subsurface baseflow based on interactions between climate and the catchment land cover characteristics. Surface runoff is calculated using the USDA SCS curve number method (Boughton, 1989), and varies as a function of land uses and soil characteristics. In the current study, curve numbers associated with watershed CORINE land use areas were extracted from the GCN 250 dataset (Jaafar et al., 2019) and a value was calculated for each land cover area based as an area-weighted mean. Baseflow is calculated as a lumped contribution from the entire watershed as both slow- and fast-moving groundwater flows (see Schneiderman et al., 2010) from three subsurface lumped reservoirs (i.e., averaged over the whole catchment): (1) the unsaturated zone (subjected to evapotranspiration), (2) a saturated zone (not subjected to

evapotranspiration), and (3) a deep saturated zone with sustained low flow discharge. Evapotranspiration is calculated within the model using the Hamon temperature index equation as default (Hamon, 1961). The original hydrology model included seven adjustable parameters to regulate the different hydrological states: (1) *precipitation correction factor*, (2) *melt coefficient*, (3) *runoff curve number adjustment*, (4) *soil water capacity*, (5) *recess coefficient*, (6) *slow recess coefficient* and (7) *baseflow capacity* (Schneiderman et al., 2010). We incorporated one additional parameter: (8) a *river channel flow coefficient* (change 1). The latter partitions surface runoff into two separate pathways: a *direct runoff* pathway and a *river channel stored discharge* pathway. With this, we aimed to represent better the timing of water flow and DOC in basins of large size and/or regulated river networks, in which water (and the DOC contained therein) is stored in the channel at times exceeding the daily time step. This stored water was subjected to evapotranspiration. A description of the model parameters for hydrology and a conceptual diagram depicting change 1 in the model structure can be found in Supp. Mat. A1.

2.2.2. DOC module

GWLF follows a two-phase process for simulating DOC concentrations at the catchment outlet: (1) DOC production and (2) DOC washout. DOC production is regulated by two processes: temperature-dependent decomposition (D_T) and moisture-dependent decomposition (D_S) of soil organic matter. In the model described by Naden et al. (2010), three adjustable parameters controlled production: (1) *activation energy* (E_a) and (2) *anaerobic decomposition rate* (a) controlled D_T, while (3) the *aerobic decomposition rate* (b) controlled D_S. Here, we assigned an independent D_T for surface land covers we defined as wetland areas (e.g., peatlands, inland marshes) for which a new separate (4) *anaerobic decomposition rate* (a_w) only was used (change 2). The aim was to account for the difference in DOC production between areas that would be subject to continual fluctuations in water level and areas which would remain water-logged, and therefore not be subjected to the same decomposition rates (Mozafari et al., 2023; Arsenault et al., 2024). Furthermore, the calculation of D_S is based on simulated soil water storage which is a basin lumped variable and which would not be representative of the conditions in water-logged areas. A description of the parameters for DOC production and a conceptual diagram depicting change 2 in the model structure can be found in Supp. Mat. A2.

The DOC produced in the original model was stored in a single carbon catchment pool and made available for washout via all runoff and groundwater flows, regulated by three parameters (Naden et al., 2010). Here, instead of using a single pool, we defined pools that mirrored the main hydrological stores (i.e., the surface soils of the catchment, the unsaturated zone, and the deeper saturated zones), and accounting for the available carbon resulting from wetlands production as well. With this change, we aimed to track more closely how the different hydrological states drive DOC production and transport in the model. Four main pools were defined as lumped carbon reservoirs (change 3): (1) DOC produced by surface wetland-like areas, (2) DOC produced by DOC-producing surface areas that are not wetlands (see Naden et al., 2010), (3) DOC produced in the catchment unsaturated zone, and (4) DOC produced in the catchment saturated zones. Consistent with the model hydrology, DOC from surface pools 1 and 2 is available for washout via runoff flows (*direct runoff* and *channel stored discharge*), while DOC from pools 3 and 4 is available for washout via baseflow (slow- and fast- moving groundwater flows). As a result, the number of parameters to regulate the DOC transport increased from three to five: (1) *surface carbon loss coefficient,* (2) *surface flow cap,* (3) *baseflow ratio,* (4) *fast groundwater flow carbon loss coefficient* and (5) *slow groundwater flow carbon loss coefficient* (see Supp. Mat. A3 for more details). Streamflow DOC concentrations and fluxes were calculated as in the original model, from the sum of all DOC contributions (kg C day^{-1}) and using the total discharge (m^3 day^{-1}) (Naden et al., 2010).

2.3. Model calibration

For calibration of the hydrology, the measured discharge datasets were divided into two periods. The first was used for calibration and the second for validation: Vattholma (1980–2011, 2012–2022) and Glenamong (2013–2018, 2019–2023). For DOC, due to lower data availability, a single period was used for calibration only: Vattholma (1992–2022) and Glenamong (2016–2023). Model performance was evaluated based on the Nash-Sutcliffe coefficient (NSE) and the coefficient of determination (r^2) (Krause et al., 2005) between daily measured and simulated discharge, DOC concentration and DOC flux.

We adopted multistep script-based calibrations to adjust the model parameters. In line with Schneiderman et al. (2010) and Naden et al. (2010), on each calibration step, target functions were defined and the Powell search-optimisation method (Zhong and Cai, 2015) within VENSIM software (Ventana Systems Inc.) was used to calibrate parameters between pre-determined ranges. The range limits were set based on previous modelling studies and relevant literature (e.g., Evans et al., 2006; Karhu et al., 2010; Naden et al., 2010; Klimek et al., 2020; Lindqvist, 2022). The target functions for hydrology included checks for daily water balance and payoffs between simulated and measured discharge, runoff and baseflow (measured runoff and baseflow based on the Arnold et al. (1995) hydrograph separation method; see Schneiderman et al., 2010). For DOC, a payoff between daily measured and simulated DOC concentration was used as the target function on each step. Model spin-up periods of four and two years were used for Vattholma and Glenamong, respectively. Details on the range for each parameter, optimisation target functions, and a summary description of the calibration scripts can be found in Supp. Mat. A4.

2.4. Model uncertainty and sensitivity

We employed the Generalised Likelihood Uncertainty Estimation (GLUE) method (Beven and Binley, 1992, 2014) to quantify model parameter uncertainty. GLUE allows the exploration of parameter uncertainty by sampling from the parameter space and evaluating model performance against observed data. First, a Monte Carlo simulation round (30,000 model runs) was performed for each catchment, varying the parameters within calibration ranges. Second, an NSE threshold of 0.60 was defined for hydrology (simulated vs measured discharge) and of 0.30 for DOC (simulated vs measured DOC concentration) respectively, as a likelihood measure to constrain parameter variability space (i.e., to further constrain the parameter ranges so that more simulations with an acceptable NSE value above the selected thresholds are output) (Pianosi et al., 2016). A second simulation round (30,000 runs) was then performed using these constrained ranges. From all parameter sets above the likelihood measure thresholds (i.e., behavioural parameter sets), the 100 best-performing sets were used to compute 5 % to 95 % range GLUE uncertainty bounds (Beven, 2009). Model equifinality (i.e., how sensitive the model is to different parameter sets that produce acceptable simulations of observed behaviour) (Beven and Freer, 2001) was assessed individually for hydrology and DOC, relative to the selected likelihood measure (i.e., the NSE metric) and using all behavioural parameter sets.

2.5. Future projections

Future climate projections for the meteorological input variables were derived from the 5-member GCM ensemble provided by the open-access Inter-Sectoral Impact Model Intercomparison Project (0.5° ISIMIP 3b simulation round; data.isimip.org) (Lange and Büchner, 2021). Grid-cell daily values of future precipitation and mean air temperature from 2021 to 2100 were extracted for each study catchment for three Shared Socioeconomic Pathways (SSP): SSP126, SSP370 and SSP585. These represent three different futures of greenhouse gas (GHG) emission levels, societal development, and adaptation to climate change

(IPCC, 2023). Ranging from a more to a less optimistic scenario, SSP126 reflects rapid efforts to mitigate GHG emissions while promoting environmental and economic sustainability, SSP370 adopts intermediate efforts for both adaptation and mitigation, and SSP585 assumes increasing trends in fossil-fuelled development i.e., a high level of human-induced global warming. In addition, a 30-year baseline period from 1985 to 2014 was defined, for which daily input data for each catchment were extracted from the historical period of the same ISIMIP3b GCMs. All ISIMIP3b data have been subject to robust statistical downscaling and bias adjustment (see Supp. Mat. A5 for more details).

2.5.1. Data processing and analysis

For each scenario simulation (baseline, SSP126, SSP370 and SSP585), one meteorological dataset for each GCM was used to drive GWLF-DOC for each of the 100 top behavioural parameter sets (see Section 2.4) so that the uncertainty associated with the different GCMs and that associated with model parameters were estimated. A daily, monthly, and annual ensemble mean of the resulting 500 simulations for each scenario (5 GCMs x 100 behavioural parameter sets) was calculated for each SSP scenario. The model outputs for the SSPs were collated for two decadal periods: 2050–2059 (P1) and 2090–2099 (P2), which were used to compare against outputs for the baseline period. Furthermore, we computed future anomalies at the annual scale (Du and Deng, 2022) from 2030 to 2100 for discharge and DOC concentration between each future scenario and the baseline. The uncertainty in the predictions was calculated as the standard deviation of the ensemble. We also displayed the likelihood that each scenario would exceed 95th percentile baseline levels for DOC concentration and flux (as metrics of current extreme conditions) in future meteorological seasons. Seasonal analyses were based on the typical three-month periods relevant for management: spring (March to May), summer (June to August), autumn (September to November) and winter (December to February). Lastly, the relative contribution of (1) future climate input data and (2) model parameterisation to the total uncertainty in predictions was assessed based on a variance partitioning procedure (Watling et al., 2015; Lofton et al., 2022). For this, the model was run with all five GCMs but using only the calibrated set of model parameters (see Section 2.3). Then, it was run using all 100 best-performing model parameter sets with each GCM dataset. A normalised difference of the variances in the simulation results was then computed to estimate individual relative uncertainty contributions (Lofton et al., 2022). The same calculations were followed for each of the two catchments.

3. Results

3.1. Model performance and uncertainty

The results from the optimisation procedure for catchment hydrology indicated a good fit at both sites. The NSE values for average monthly and daily discharge based on the best optimised simulation ranged from 0.73 to 0.79 for Vattholma, and from 0.60 to 0.78 for Glenamong (Figs. 2a and B1a). Similarly, r^2 values ranged from 0.76 to 0.80 for Vattholma, and from 0.60 to 0.78 for Glenamong (Figs. 2b and B1b). For DOC, the metrics for the best optimised simulation were higher for DOC fluxes than for DOC concentrations at both sites. For Vattholma, the NSE and r^2 values for the daily DOC flux were 0.73 and 0.74 respectively, while those for daily DOC concentration were 0.39 and 0.39 (Fig. 3a and c). For Glenamong, the NSE and r^2 values for daily DOC flux were 0.60 and 0.62, while those for daily DOC concentration were 0.45 and 0.47 respectively (Fig. 3b and d). Simulated DOC flux for each study site reflected site-specific dynamics and intra-annual variations (Fig. B2a and b). Baseflow was a major contributor to both

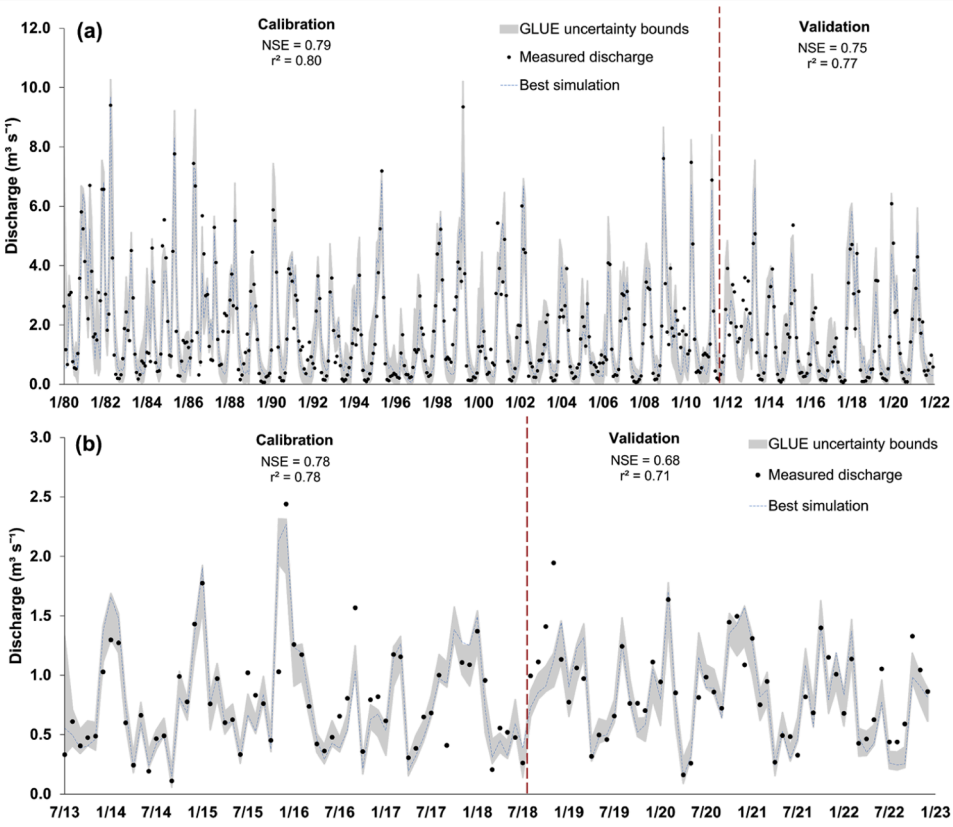

Fig. 2. Observed and simulated monthly river discharge for Vattholma (a) and Glenamong (b) catchments during model calibration and validation. NSE and r^2 values are indicated for the calibrated parameter set (best optimised simulation). The grey area denotes the 5–95 % range GLUE uncertainty bounds for river discharge based on the 100 best-performing parameter sets.

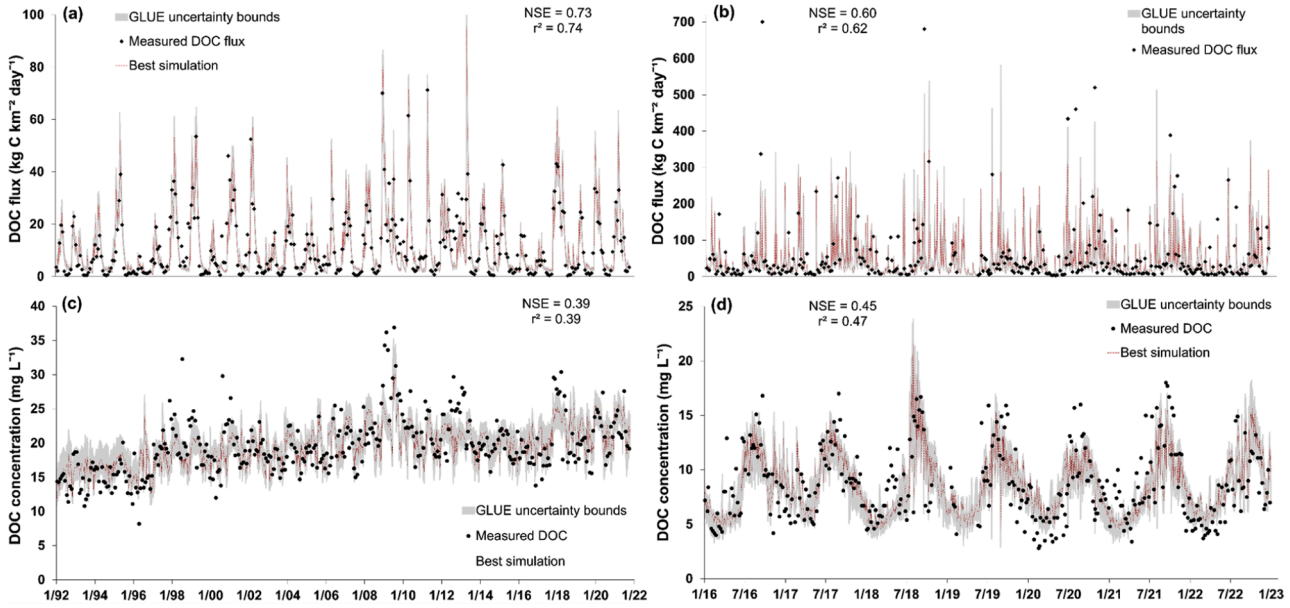

Fig. 3. Observed and simulated daily DOC flux and DOC concentrations for Vattholma (a and c) and Glenamong (b and d) catchments during model calibration. NSE and r^2 values are indicated for the calibrated parameter set (best optimised simulation). The grey area denotes the 5–95 % range GLUE uncertainty bounds for DOC flux and DOC concentrations based on the 100 best-performing parameter sets.

discharge (Fig. B2c–f) and carbon export in Vattholma, while there was a more balanced ratio between baseflow and surface runoff for Glenamong.

The set of calibrated model parameters obtained for the best optimisation run reflected the differences between the study sites (Table B1). Except for the precipitation correction factor and soil water capacity, the optimised values for the hydrological parameters were generally higher for Glenamong than for Vattholma, particularly the river channel flow coefficient. For DOC production, the optimisation resulted in a higher activation energy (E_a = 6.4) and aerobic decomposition rate (b = 7.4) for Vattholma, indicating a greater sensitivity to changes in soil temperature and moisture levels at this site than for Glenamong (E_a = 3.0 and b = 1.0). In contrast, the values for both anaerobic decomposition rates were an order of magnitude greater at the Glenamong, reflecting the importance of saturation of the deep Irish peat soils. In terms of DOC transport, the optimised values for the Glenamong reflected a larger contribution of surface runoff at that site, with higher values for the runoff carbon loss coefficient and surface flow cap than for Vattholma. Subsurface carbon transport through fast groundwater flow was favoured over slow groundwater flow at both sites, with both optimisations also indicating relatively low groundwater carbon loss coefficients.

The GLUE uncertainty bounds captured a similar level of variation in measured discharge and DOC concentration to that captured by the optimisation process, but allowed for a range of parameter values rather than a single optimised set (Table B1). For discharge, 73 % and 60 % of the measured monthly observations and 65 % and 50 % of the daily observations were captured by the uncertainty bounds for Vattholma (Figs. 2a and B1a) and Glenamong (Figs. 2b and B1b) respectively, while the values for DOC concentration were 45 % and 38 % (Fig. 3c and d). Furthermore, sensitivity plots showed that the DOC model was typically more sensitive to parameter variation than the hydrology model (Figs. B3–B6). Discharge was sensitive to the value of the precipitation correction factor for both sites, and insensitive to the value used for baseflow capacity and soil water capacity (i.e., acceptable model performance occurred over the entire parameter range). Parameters related to flow attenuation (recess coefficient, slow recess coefficient and melt coefficient) were sensitive only at Vattholma. In contrast, parameters more related to catchment surface water retention (runoff curve number adjustment and river channel flow coefficient) were more sensitive for Glenamong. Parameters related to DOC production were sensitive for both catchments except for activation energy at Vattholma, where a wide range of values produced an equally good fit. Similarly, parameters related to DOC transport were sensitive at both sites, although the surface flow cap displayed less sensitivity (i.e., acceptable performance over a large extent of its parameter range).

3.2. Future climate impacts

The GCM ensemble for all three future SSP scenarios projected changes in climatic conditions for each site relative to their baseline periods (Table 2; Fig. 4a–d) (Tables B2–B13 show conditions projected by each GCM ensemble member). Large air temperature increases were projected for Vattholma, ranging from +1.5 °C (+24 %; SSP126) to +6.0 °C (+95 %; SSP585) across the scenarios. However, SSP126, the scenario that incorporates some mitigation effects, was the only scenario for which temperature first increased in P1 (2050–2059) (+2.1 °C; +33 %) and then decreased in P2 (2090–2099) (+1.5 °C; +24 %). For the Glenamong, there was only a slight increase in air temperature for projections based on SSP126 in both P1 (+0.4 °C; +4 %) and P2 (+0.2 °C; +2 %). In contrast, the ensemble mean for SSP370 and SSP585 indicated much warmer conditions during both P1 (up to +12 %) and P2 (up to +33 %). Under SSP585, it was of note that, although similar annual air temperatures were projected for both sites in the final decade of the century (Vattholma: 12.3 °C; Glenamong: 12.2 °C), this represented a more extreme increase at the Swedish site (+6.0 °C; +95 %) than at the Irish site (+3.0 °C; +33 %).

Annual precipitation was also projected to increase in Vattholma under all scenarios during both P1 and P2 (Table 2). However, the increases were, in relative terms, less extreme than those for temperature. They ranged by up to +10 % in P1 and +15 % in P2. The largest increase in that latter period was actually projected for SSP370 (+108 mm yr^{-1}). Smaller relative increases in annual precipitation were projected for Glenamong, up to +2 % in P1 and +8 % in P2. In fact, for Glenamong, where annual precipitation was already over twice that at Vattholma for the baseline period (1710 mm yr^{-1} versus 712 mm yr^{-1}, respectively), all projections were similar to the baseline with the exception for SSP585 in P2 (+136 mm yr^{-1}). There was, however, a pronounced

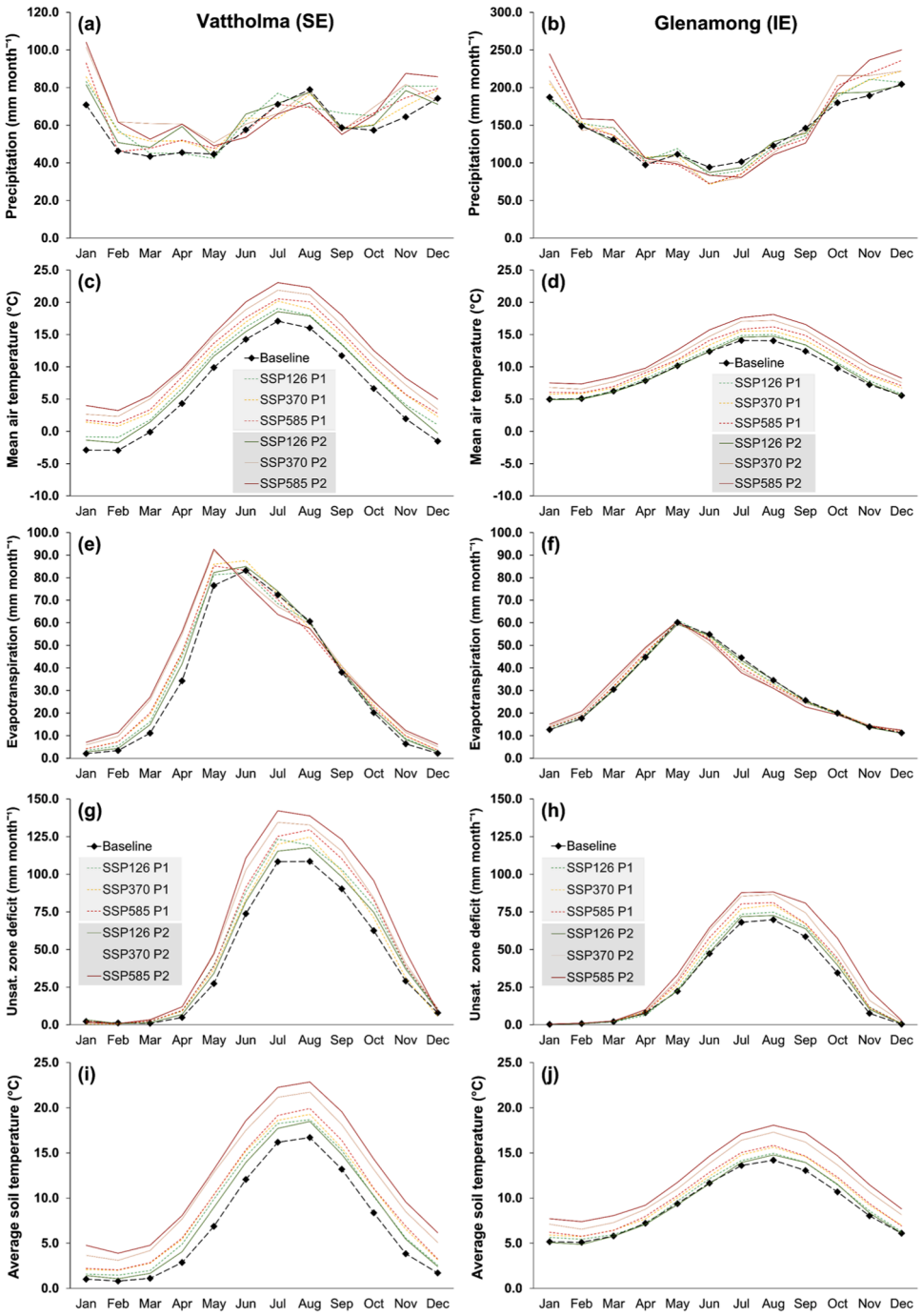

Fig. 4. ISIMIP3b GCM-ensemble average monthly precipitation (a and b), ISIMIP3b GCM-ensemble mean air temperature (c and d), average modelled monthly actual evapotranspiration (e and f), average modelled unsaturated zone deficit (g and h) and average modelled soil temperature (i and j) for the baseline period and for the SSP126, SS370 and SSP585 scenarios during P1 and P2. Note the different scaling in panels a and b. Vattholma: a, c, e, g, i; Glenamong: b, d, f, h, j.

seasonal shift in precipitation at the Irish site, with generally drier conditions than the baseline period between April and September, and wetter conditions between October and March (Fig. 4a and b). At Vattholma, future precipitation was clearly elevated in the autumn and winter from October to March, but the direction of change projected by the different CGMs varied in other months. The variability in future climate, indicated by the standard deviation, increased by the end of the century at both sites and was highest under SSP585 (Table 2).

The future changes in evapotranspiration reflected the changes in both air temperature and precipitation (Fig. 4e and f). In general, higher monthly actual evapotranspiration was projected from October to May at both sites, followed by decreases from June to September, although the changes were greater at Vattholma.

3.3. Future change in discharge

There were pronounced changes in seasonal discharge patterns, especially for Vattholma during the first six calendar months (Fig. 5a). Most noticeable was that, except for SSP126 in P1, the peak month for discharge shifted to earlier in the year, with increased discharge from January to March particularly in P2 (+63 %; SSP585). These increases were followed by decreases in discharge from April to June under all three scenarios, with the lowest levels in P2 as well (up to −38 %; SSP585). There was a slight upward shift in daily discharge magnitudes

Table 2
ISIMIP3b GCM ensemble-mean future annual precipitation and mean air temperature values for the historical period (baseline) and for the SSP126, SSP370 and SSP585 scenarios during P1 (2050–2060) and P2 (2090–2100), for each study catchment. The standard deviation is indicated in parentheses.

	Vattholma (SE)		Glenamong (IE)	
Period	Mean air temperature (°C)	Precipitation (mm yr^{-1})	Mean air temperature (°C)	Precipitation (mm yr^{-1})
Baseline (1985–2014)	6.3 (±1.1)	712 (±100)	9.2 (±0.5)	1710 (±171)
SSP 126				
P1 (2050–2059)	8.4 (±1.0)	730 (±116)	9.6 (±0.7)	1728 (±162)
P2 (2090–2099)	7.8 (±1.6)	764 (±142)	9.4 (±1.2)	1715 (±182)
SSP 370				
P1 (2050–2059)	9.1 (±1.3)	782 (±116)	10.2 (±0.7)	1749 (±204)
P2 (2090–2099)	11.3 (±2.2)	820 (±136)	11.4 (±1.6)	1763 (±184)
SSP 585				
P1 (2050–2059)	9.3 (±1.4)	764 (±109)	10.3 (±0.9)	1737 (±227)
P2 (2090–2099)	12.3 (±2.5)	812 (±145)	12.2 (±1.9)	1846 (±224)

for SSP126 during the last decade of the century, while values for SSP370 and SSP585 were similar to those during P1 but with more variability (Fig. 5b). In the Glenamong, the projections indicated that discharge would be relatively unchanged under SSP126 (Fig. 5d). In contrast to the Swedish site, it was projected to decrease from April to September followed by increased levels from October to March under SSP370 and SSP585. The decreases were greatest for July in P1 (up to −25 %; SSP370) and the largest increases in discharge were for January in P2 (up to +30 %; SSP585). There was little change in the magnitude of discharge at the daily timescale for the Glenamong in both P1 and P2 under all three scenarios, although SSP585 had a greater range of values (Fig. 5e).

Ensemble mean annual discharge anomalies for Vattholma sometimes contrasted between future scenarios, but were all similar in magnitude: up to ±1.1 $m^3\ s^{-1}$ under SSP126, up to ±1.3 $m^3\ s^{-1}$ under SSP370, and up to ±1.1 $m^3\ s^{-1}$ under SSP585 relative to a baseline average of 2.4 $m^3\ s^{-1}$ (Fig. 5c). For Glenamong, discharge anomalies were lower in magnitude than for the Swedish site but greatest for SSP585 (up to ±0.2 $m^3\ s^{-1}$) than for SSP126 and SSP370 (up to ±0.1 $m^3\ s^{-1}$) relative to a baseline average of 0.6 $m^3\ s^{-1}$ (Fig. 5f). At each of the study sites, all three future projections displayed a similar uncertainty range throughout the simulation, which slightly increased towards the end of the century (Fig. 5c and f).

3.4. Future change in DOC concentrations and flux

The variables that drive carbon decomposition in the model also showed large changes in the future, with increases projected in soil temperatures (reflecting higher air temperature), and a drier soil matrix in summer (reflecting both increases in evapotranspiration and lower precipitation in summer) (Fig. 4g–j). Conditions that would be expected to increase decomposition and ultimately stream DOC concentration.

The simulations indicated that DOC concentrations would increase for Vattholma throughout the calendar year under all three SSPs (Fig. 6a). In P1, these increases ranged from +4 mg L^{-1} (SSP370) to +6 mg L^{-1} (SSP585) (baseline average of 13.7 mg L^{-1}). In P2, even larger increases were projected, particularly for SSP370 and SSP585, exceeding baseline levels by up to +9 mg L^{-1}. However, it is of note that the increases projected for SSP126 were lower in P2 (up to +3 mg L^{-1}) than those for all scenarios in P1. A clear general upward shift in the magnitude and minimum DOC concentration was indicated for all three scenarios (Fig. 6b). Again, the levels projected using SSP126 were closer to the baseline by the end of the century. DOC variability was also projected to increase, especially in P2 under SSP370 and SSP585. Ensemble mean annual DOC concentration anomalies for Vattholma were always positive, that is they were always higher than the historical baseline, in the order of ≃ +3, +4 and +5 mg L^{-1} for SSP126, SSP370 and SSP585, respectively (Fig. 6c). The anomalies continued to increase until the end of the century under both SSP370 and SSP585, while those for SSP126 decreased after 2060. The output for SSP126 also had the lowest uncertainty range, while that for SSP585 was the largest, particularly during P2, projecting futures with extremely high annual DOC concentrations of up to +13 mg L^{-1} above the baseline mean.

DOC concentrations were also projected to increase for Glenamong in all months under all three SSPs (Fig. 6d). The lowest increases were for SSP126, and were similar in P1 and in P2 (≃ +1 mg L^{-1}) (baseline average of 9.2 mg L^{-1}). The concentrations projected under SSP370 and SSP585 were larger, particularly from July to November in P2, exceeding baseline levels by ≃ +4 mg L^{-1}. A small upward shift in the magnitudes and variability of DOC concentrations relative to the baseline was projected in P1 under all three scenarios (Fig. 6e). In P2, the magnitude and variability increased more under SSP370 and SSP585 but, as with Vattholma, decreased under SSP126. Ensemble mean annual DOC concentration anomalies were also consistently positive for Glenamong in the order of ≃ +0.6, +1.0 and +1.3 mg L^{-1} for SSP126, SSP370 and SSP585, respectively (Fig. 6f). The anomalies increased over time under SSP370 and SSP585, while SSP126 anomalies decreased after 2070. Uncertainty increased with time under all three scenarios, with SSP126 displaying the narrowest range. SSP585 projections were the most uncertain, with anomalies of up to +5 mg L^{-1} over the last decade.

The probabilities of exceeding the 95th percentile baseline DOC concentration level (a metric of current extreme conditions) were much higher for Vattholma during each season than for Glenamong under all three future climate scenarios (Fig. 7). In line with other results, extreme DOC concentrations for Vattholma were lowest for SSP126 than for the other two scenarios, and therefore the probabilities of exceeding the historical 95th percentile threshold concentration of 15 mg L^{-1} were also lower across seasons (Fig. 7a). In particular, increases in the likelihood of occurrence for extreme concentrations were projected for all seasons under SSP370 and SSP585, while spring and winter were the most affected under SSP126. For Glenamong, in contrast, the probability of exceeding the baseline 95th percentile DOC concentration threshold of 13 mg L^{-1} were zero during the spring and winter under all three scenarios (Fig. 7b). However, there was an increased probability for exceeding this threshold in the summer and even higher probability of exceedance for the autumn under all three scenarios but higher under SSP370 and SSP585.

Furthermore, extreme DOC concentrations for Vattholma were projected to be accompanied by an increasing likeliness of extreme DOC flux in spring and winter under all three scenarios, while the summer and autumn were not affected (Fig. B7a). For Glenamong, the likelihood of occurrence for extreme DOC flux was virtually zero across seasons under all three SSPs (Fig. B7b).

3.5. Uncertainty partitioning

In all projections for both river discharge and DOC concentration, the uncertainty (indicated by the standard deviation) typically increased with time and the relative contribution of the future climate driving data

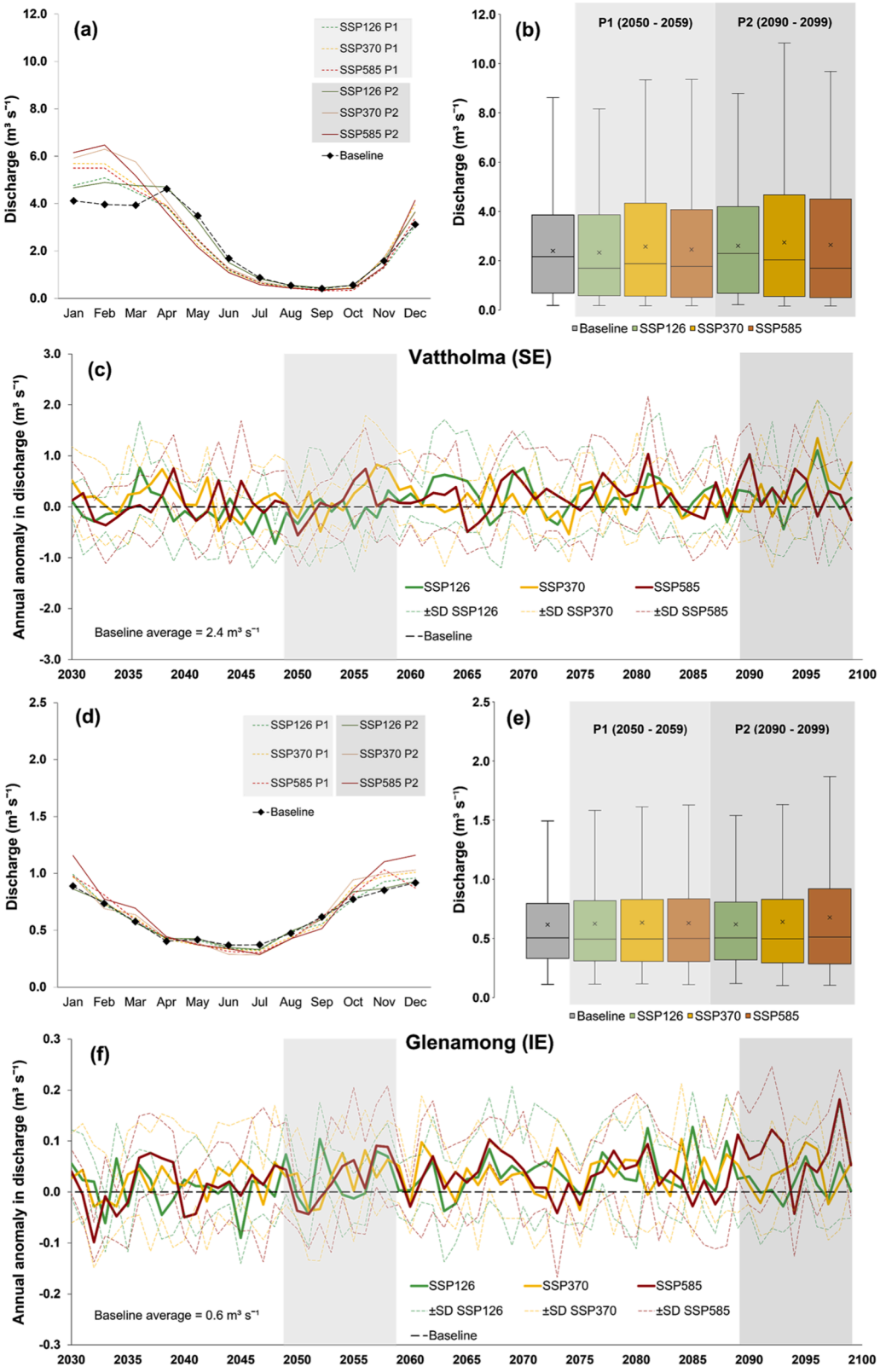

Fig. 5. Average calendar month discharge (a and d); boxplot distributions of average daily discharge for the baseline period, and for the SSP126, SS370 and SSP585 scenarios during P1 and P2 (b and e); annual anomalies for discharge under SSP126, SS370 and SSP585 scenarios from 2030 to 2100 (c and f). Uncertainty in the discharge anomaly panels is indicated by the standard deviation (±SD) and delimited by SSP126, SS370 and SSP585 legend colour dotted lines respectively. Vattholma: a, b, c; Glenamong: d, e, f.

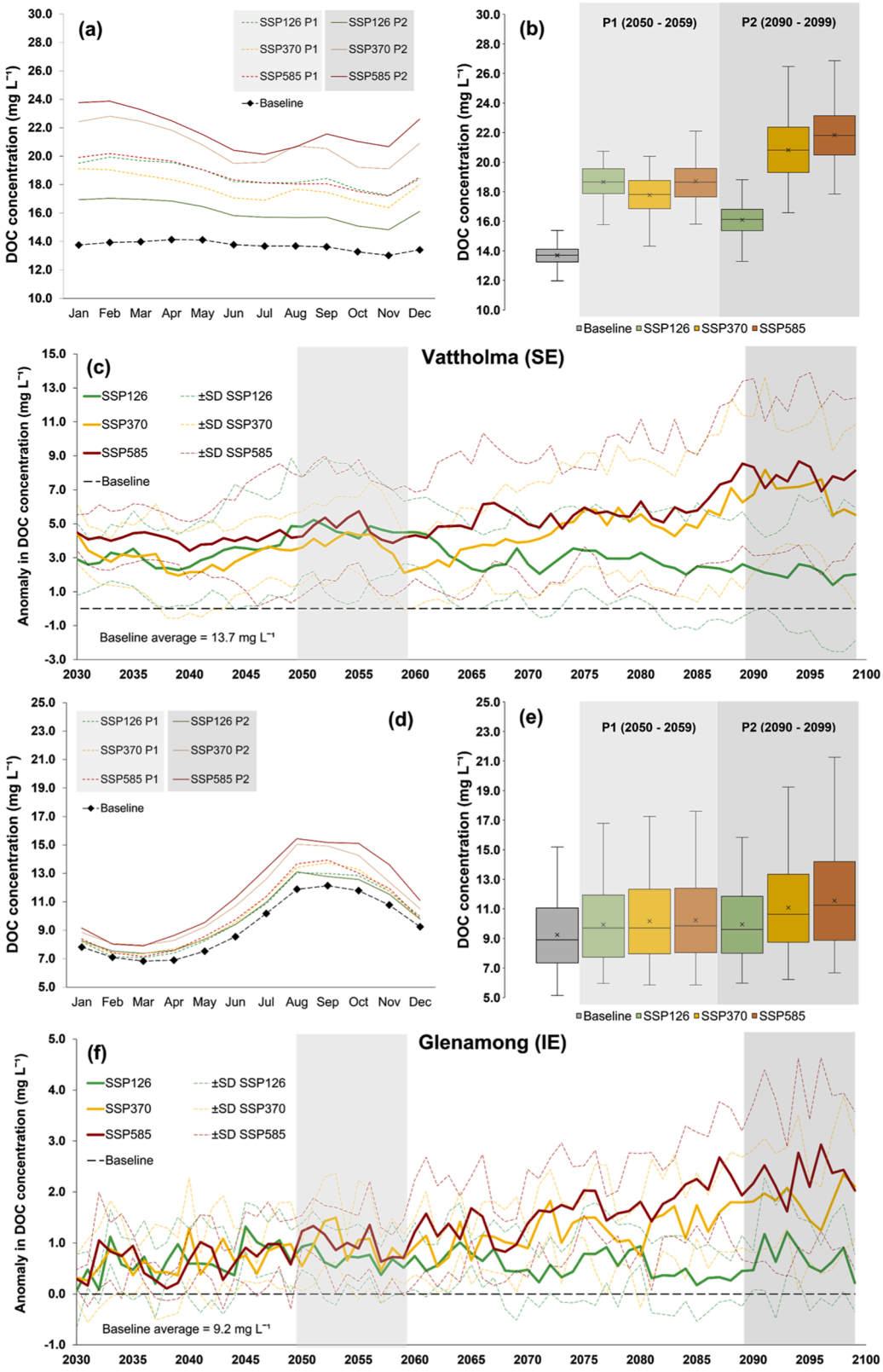

Fig. 6. Average calendar month DOC concentration (a and d); boxplot distributions of average daily DOC concentrations for the baseline period, and for the SSP126, SS370 and SSP585 scenarios during P1 and P2 (b and e); annual anomalies for DOC concentration under SSP126, SS370 and SSP585 scenarios from 2030 to 2100 (c and f). Uncertainty in the DOC concentration anomaly panels is indicated by the standard deviation (±SD) and delimited by SSP126, SS370 and SSP585 legend colour dotted lines respectively. Vattholma: a, b, c; Glenamong: d, e, f.

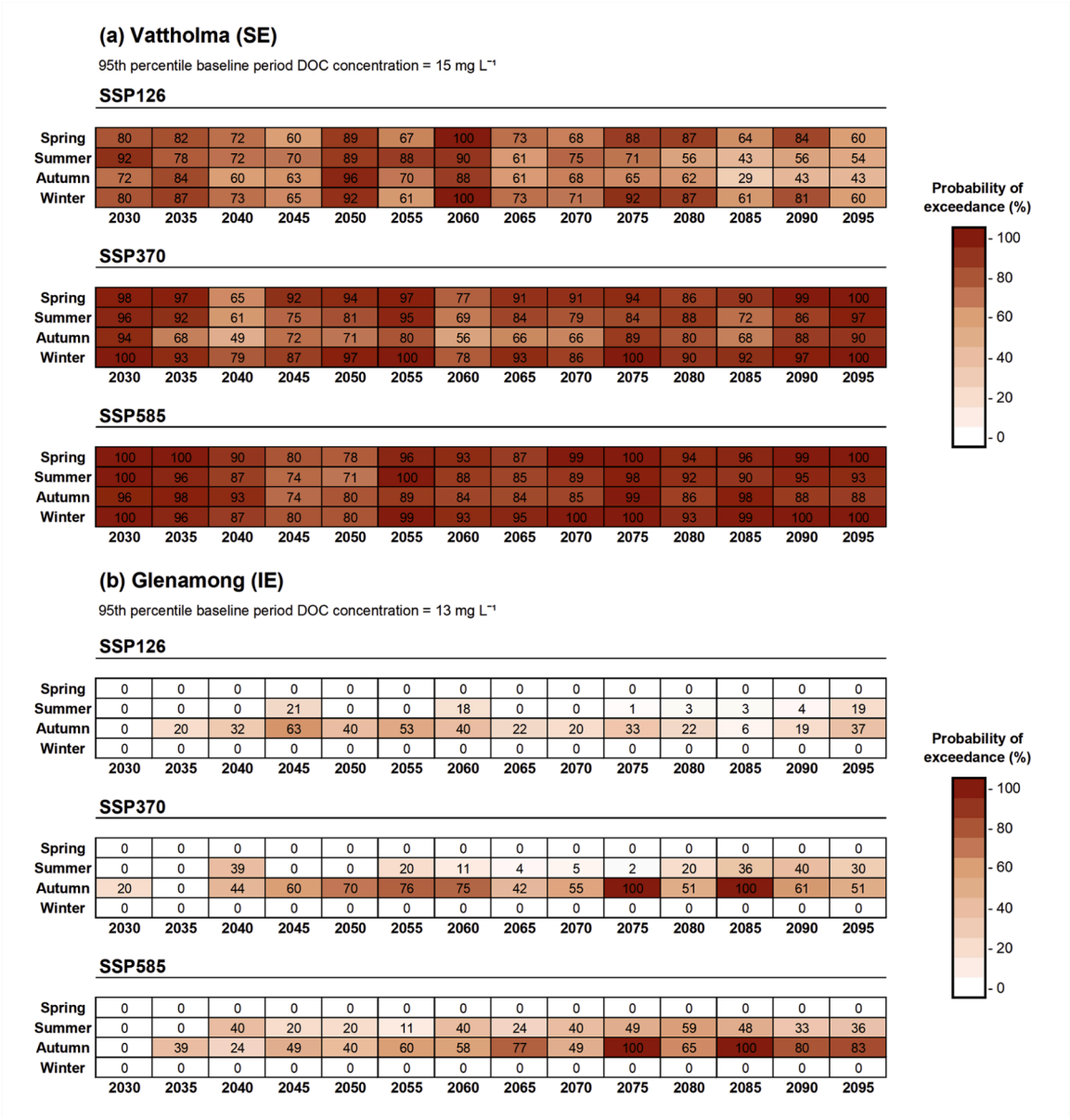

Fig. 7. Tercile plots displaying the probability of exceeding the 95th percentile baseline DOC concentration (mg L^{-1}) for each typical meteorological season (spring, summer, autumn and winter) in the future (every 5 years) under SSP126, SSP370 and SSP585 scenarios for Vattholma (a) and Glenamong (b). The shading of each square represents the probability of exceedance based on the categorised colour bar legend. The ensemble size was comprised of 500 members for each scenario.

(i.e., for the five GCMs) to total uncertainty was generally much larger than the contribution of model parameterisation (i.e., for the 100 behavioural parameter sets) (Figs. 8 and B8). Variation between GCMs made the greatest contributions (up to 85 %) to total uncertainty for all discharge simulations, although the hydrological model parameters accounted for a greater percentage of variation in simulation for Vattholma than for Glenamong (Fig. B8). For DOC concentrations, future climate data were also the most important source of uncertainty, but of note were the higher contributions from the DOC model parameters for the Swedish site (Fig. 8). These were relatively large, particularly under SSP370 and SSP585, and at times contributed up to 50 %. In contrast, the DOC model parameters contributed much less to the uncertainty in DOC projections for the Glenamong, especially under SSP585.

4. Discussion

Implementing adaptive management in response to the impacts of global warming is becoming more and more critical as records of climatic extremes continue to be exceeded (Ripple et al., 2023; Esper et al., 2024). These changes are having profound impacts on water quantity and quality (van Vliet et al., 2023), including on the DOC concentration in drinking source waters and therefore potentially on the formation of DBPs (Absalan et al., 2024). In order to respond and adapt, water managers require robust estimates of future change from the modelling community. Our projections for two contrasting catchments, in regions were DBP formation is already an issue, show that DOC concentrations are projected to show large increases, with the highest levels related to scenarios where mitigation is not addressed. They also highlight the importance of incorporating model parameter uncertainty into the future projections, a source of uncertainty that is often omitted. This is especially important for model parameters such as those related to carbon decomposition and transport in organic soils, that will respond directly to variations in temperature and water availability.

Our results relative to many recent studies (e.g., Futter et al., 2011; Son et al., 2019; Xu et al., 2020) have a similarly good or better model performance, especially for modelling DOC concentration. The future

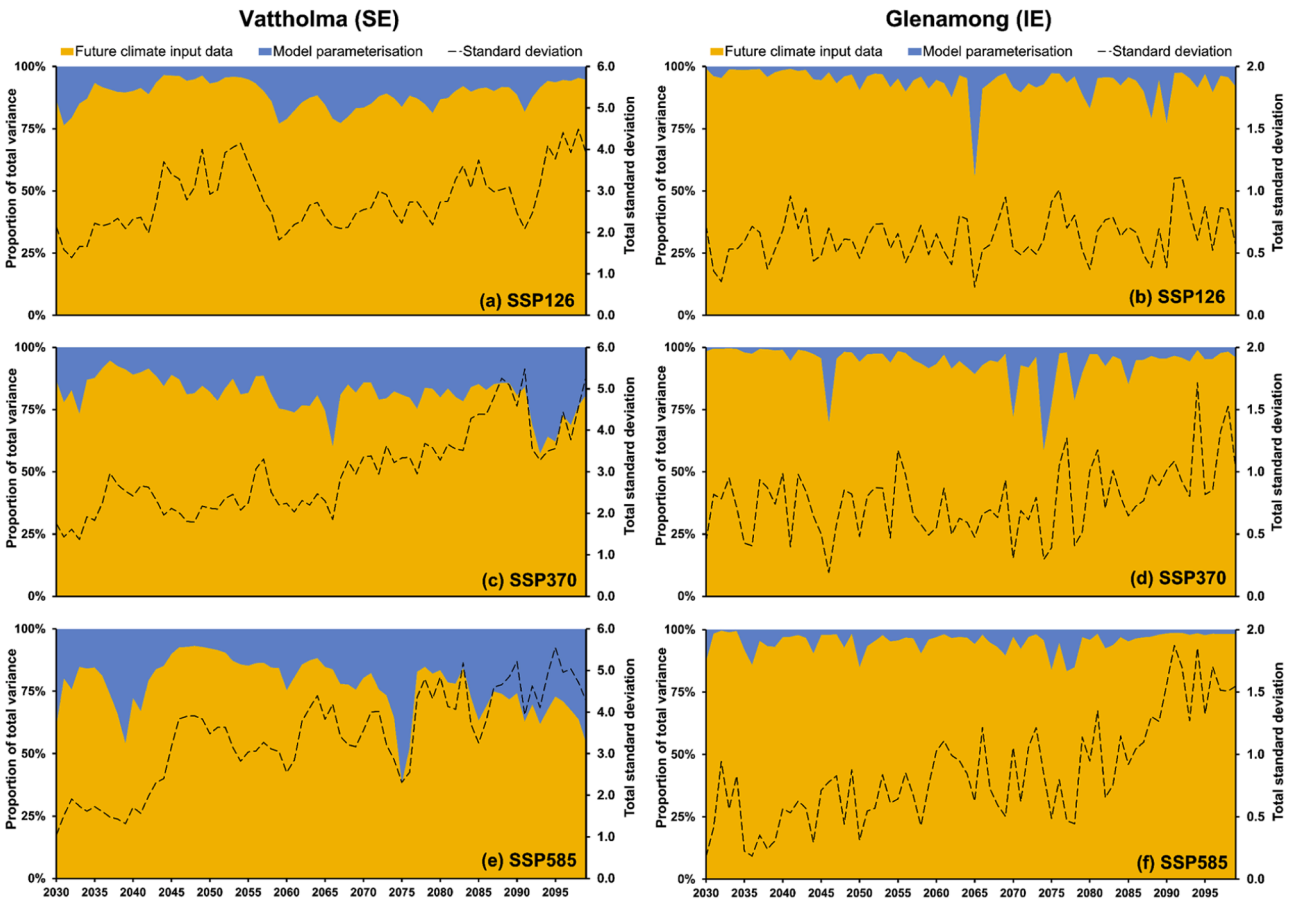

Fig. 8. Relative contribution of (1) future climate input data and (2) model parameterisation as individual sources of uncertainty to the total uncertainty in future projections of DOC concentration under SSP126, SSP370 and SSP585 scenarios for Vattholma (a, c, and e) and Glenamong (b, d and f).

changes quantified for river discharge and DOC concentration in this study also lie in a similar order of magnitude to those projected in other research for these sites (e.g., Naden et al., 2010; Lindqvist, 2022). That is, discharge projections indicate both decreasing and increasing levels under different scenarios depending on the time scale, season and context. In terms of DOC, the overall picture is for an increase in concentration and flux with different magnitudes depending on the study site and scenario. It is important to be aware, however, that these results should not be compared directly to the work of others without acknowledging the differences in modelling approach. These include changes in model structure, driver data type (e.g., stationary projections compared to transient GCM-driven projections), future scenario conditions, and the examination here of effects related to model parameterisation.

Although accounting for model parameterisation can result in simulations with larger uncertainty (Schürz et al., 2019), this is generally outweighed by producing a more accurate range of variability for the modelled variables (Her et al., 2019b; Marshall et al., 2021). Furthermore, by partitioning the total uncertainty of the predictions, we have quantified the impacts of this parameterisation on long-term projections for river discharge and DOC concentration (Figs. 8 and B8). While the GCM ensemble was the dominant source of uncertainty, a finding in line with many other climate change impact assessments (Hattermann et al., 2018; Kundzewicz et al., 2018), the variability in DOC model parameterisation was also important for some of our simulations. This was the case for the Vattholma catchment in Sweden under all three SSPs. An important contributing factor to this was that the behavioural ranges of key soil decomposition parameters (i.e., activation energy (E_a) and aerobic decomposition rate (b)) were higher in magnitude for this site than for the Irish site. This led to the parameters showing larger responses to increasing temperatures and changes in soil moisture levels in the Swedish catchment, and in turn to larger uncertainty contributions, particularly under SSP370 and SSP585. This also led to such large increases projected for DOC concentration at that site under these two scenarios (see Fig. 6a), as the response of these parameters likely translated to a higher amount of DOC produced in the soil matrix and, therefore, to a higher DOC export.

Determining the relative importance of model parameterisation versus future climate inputs can inform efforts to reduce total uncertainty in such projections. In GCM-driven projections for water resources, improving the quality of climate data, increasing GCM ensemble size, and better spatial and temporal input resolution are often indicated as the most effective steps (Hattermann et al., 2018; Kundzewicz et al., 2018; Her et al., 2019b). However, when model parameter uncertainty plays an important role, improving catchment model structure and parameter representation for both hydrology and water quality should also be evaluated (Schürz et al., 2019; Marshall et al., 2021). Using as an example the model structure of GWLF-DOC, these actions could be focused on the parameters that showed the greatest sensitivity (see Section 3.1).

Moreover, although other potential sources of uncertainty were not included (e.g., methods for bias correction, use of an ensemble of catchment models, land use change projections, and input data downscaling), this study represents a step forward in catchment DOC water quality modelling. By incorporating model parameter uncertainty, all of our results including those representing the likelihood of extreme DOC concentration and DOC flux account, to a large extent, for model equifinality. This key aspect is required for a better interpretation of the results (Naden et al., 2010), especially of DOC model outputs that were produced using a model structure forced by hydrology (Wei et al., 2024).

It is to note, however, that GWLF-DOC does not replicate other factors that influence DOC dynamics such as those related to biochemistry in soils (e.g., pH response and microbial populations) or in-stream processes. Nevertheless, we consider it captured the fundamental processes related to temperature and water availability variations in the soil that drive DOC dynamics at the catchment scale.

4.1. Implications for water management

Our simulations quantify the DOC concentration envelope within which water managers at similar sites may need to operate in the future. Such results could be used to evaluate scenario-based management for preserving source water quality and supply. It was clear, however, that the SSP126 scenario represented the best trajectory in terms of future change, not only for climate but also for DOC source waters. Higher and more variable concentrations, and the likelihood of extremes, were much smaller under this scenario, especially over the long term. Moreover, a process-based modelling approach such as that described can provide insights into how climate and other key catchment dynamics influence DOC concentrations at the outlet. This allows the identification of site-specific measures to reduce DOC thereby safeguard drinking water in the context of DBPs both by catchment management or improved water treatment.

Catchment-scale measures could include improved soil management, riparian buffers, land use regulations, soil treatment, drain-blocking in peatlands, and preservation of organic soils (Ritson et al., 2014; Kritzberg et al., 2020; Anderson et al., 2023). These could be implemented in a targeted way for a specific hydrological zone or land cover (Xu et al., 2018; Williamson et al., 2023). At the treatment scale, understanding the magnitude of future increases could allow planning for mitigation measures, for example, improved DOM removal during pretreatment (Anderson et al., 2023) and enhanced disinfection during treatment and post-treatment (Xiao et al., 2024). Both catchment and treatment scale measures could be applied for a particular time of the year, for a management period (e.g., 5 years), or implemented gradually over the years (Anderson et al., 2023; Williamson et al., 2023). They can also be conducted while closely monitoring key variables at the water source intake (e.g., meteorology, discharge, DOC) and intensified accordingly during periods of rising DOM, such as a particular season, flow regime, or event (e.g., a drought) (Warner and Saros, 2019; Srivastav et al., 2020; Xiao et al., 2024).

At our Swedish site Vattholma, the elevated river discharge and DOC loading projected in the winter and spring may pose additional challenges, along with increased DOC concentrations. Higher amounts of carbon export would have implications downstream for Lake Mälaren that further complicate current water treatment (Köhler et al., 2016) and DBP reduction (Andersson, 2021) during these seasons. Moreover, our results indicated that groundwater flow pathways play a critical role in DOC export for this site. This finding has also been highlighted for other Swedish sites in other modelling studies (Naden et al., 2010; Jutebring Sterte et al., 2022). Therefore, extra attention could be paid to measures that consider the saturated sub-surface zone, its impacts on baseflow and the transport of DOC in the porous media including sorption-related processes (Ploum et al., 2020).

The Glenamong (Ireland) represents catchments that face a challenge directly associated with the sensitivity of a peatland-dominated land cover to climate-induced DOC release (Jennings et al., 2010; Mozafari et al., 2023). Here, the largest increases in DOC concentration, combined with a lower discharge, were indicated for the summer and autumn especially under warmer, drier scenarios. Both surface runoff and baseflow were equally important for DOC export in this catchment, emphasizing the role of the peaty topsoil not only for organic carbon decomposition (Arsenault et al., 2024) but also for transport (Prijac et al., 2023). Moreover, maximum DOC concentrations (indicated by increases and extreme events) would have a pronounced seasonality, peaking in the autumn (Fig. 7). This volatility, in particular, could represent an important challenge for water treatment (Klante et al., 2022; Riyadh and Peleato, 2024) that, along with other climate-induced impacts on catchment dynamics (Jennings et al., 2009), can further complicate Irish water supply in complying with European Union regulations, especially in the context of DPBs (O'Driscoll et al., 2018b). Management steps should, therefore, evaluate not only reducing the potential DOC increases over monthly to annual time scales but also account for high levels of temporal variability associated with extreme events (Jennings et al., 2020).

5. Conclusions

Our study has highlighted the dominant impacts of future climate variability on the uncertainty in future projections of catchment discharge and DOC dynamics. However, it also showed how model parameterisation can be an important source of uncertainty in climate change impact assessments. Importantly, DOC concentrations for our study sites were projected to increase in all simulated futures, sometimes to levels that can largely exceed the historical reference. It is of note, however, that the smallest increases and variability were estimated under SSP126, especially by the end of the century. This suggests, with regard to catchment DOC export and potentially for drinking water supply, that it might be worth adopting more long-term sustainability actions aligned with that scenario (e.g., efforts for climate adaptation, infrastructure development, and a reduction in GHG emissions). We propose that the use of our site-specific findings can assist in developing mitigation protocols and strategies that can lead to a more adaptive catchment and water treatment management.

CRediT authorship contribution statement

Ricardo Paíz: Writing – review & editing, Writing – original draft, Visualization, Software, Methodology, Formal analysis, Data curation, Conceptualization. **Donald C. Pierson:** Writing – review & editing, Validation, Supervision, Software, Resources, Methodology, Formal analysis, Conceptualization. **Klara Lindqvist:** Software, Methodology, Data curation. **Pamela S. Naden:** Writing – review & editing, Software. **Elvira de Eyto:** Writing – review & editing, Resources, Investigation, Data curation. **Mary Dillane:** Resources, Investigation, Data curation. **Valerie McCarthy:** Writing – review & editing, Supervision. **Suzanne Linnane:** Writing – review & editing, Supervision. **Eleanor Jennings:** Writing – review & editing, Validation, Supervision, Software, Resources, Project administration, Methodology, Funding acquisition, Formal analysis, Data curation, Conceptualization.

Declaration of competing interest

The authors declare that they have no known competing financial interests or personal relationships that could have appeared to influence the work reported in this paper.

Acknowledgements

This research has been funded by the inventWater Innovative Training Network (ITN) (Inventive forecasting tools for adapting water quality management to a new climate) through the European Union's Horizon 2020 research and innovation programme, under the Marie Sklodowska-Curie grant agreement no. 956623. Special thanks to the Marine Institute, the Swedish Meteorological and Hydrological Institute (SMHI), and the Swedish Agricultural University (SLU) for their efforts in data monitoring and collection

Supplementary materials

Supplementary material associated with this article can be found, in the online version, at doi:10.1016/j.watres.2025.123238.

Data availability

Data will be made available on request.

References

Absalan, F., Hatam, F., Prévost, M., Barbeau, B., Bichai, F., 2024. Climate change and future water demand: implications for chlorine and trihalomethanes management in water distribution systems. J. Environ. Manag. 355, 120470. https://doi.org/10.1016/j.jenvman.2024.120470.

Adler, T., Underwood, K.L., Rizzo, D.M., Harpold, A., Sterle, G., Li, L., Wen, H., Stinson, L., Bristol, C., Stewart, B., Lini, A., Perdrial, N., Perdrial, J.N., 2021. Drivers of dissolved organic carbon mobilization from forested headwater catchments: a multi scaled approach. Front. Water 3, 578608. https://doi.org/10.3389/frwa.2021.578608.

Anderson, L.E., DeMont, I., Dunnington, D.D., Bjorndahl, P., Redden, D.J., Brophy, M.J., Gagnon, G.A., 2023. A review of long-term change in surface water natural organic matter concentration in the northern hemisphere and the implications for drinking water treatment. Sci. Total Environ. 858, 159699. https://doi.org/10.1016/j.scitotenv.2022.159699.

Andersson, A., 2021. Uncharted Waters: non-target analysis of disinfection by-products in drinking water. Linköping Studies in Arts and Sciences. Linköping University Electronic Press, Linköping. https://doi.org/10.3384/diss.diva-173312.

Arnold, J.G., Allen, P.M., Muttiah, R., Bernhardt, G., 1995. Automated base flow separation and recession analysis techniques. Groundwater 33, 1010–1018. https://doi.org/10.1111/j.1745-6584.1995.tb00046.x.

Arsenault, J., Talbot, J., Moore, T.R., Knorr, K.-H., Teickner, H., Lapierre, J.-F., 2024. Patterns and drivers of organic matter decomposition in peatland open-water pools. https://doi.org/10.5194/egusphere-2024-271.

Büttner, G., Kosztra, B., Soukup, T., Sousa, A., Langanke, T., 2017. CLC2018 Technical guidelines.

Beven, K., Binley, A., 1992. The future of distributed models: model calibration and uncertainty prediction. Hydrol. Process. 6, 279–298. https://doi.org/10.1002/hyp.3360060305.

Beven, K., Binley, A., 2014. GLUE: 20 years on. Hydrol. Process. 28, 5897–5918. https://doi.org/10.1002/hyp.10082.

Beven, K., Freer, J., 2001. Equifinality, data assimilation, and uncertainty estimation in mechanistic modelling of complex environmental systems using the GLUE methodology. J. Hydrol. 249, 11–29. https://doi.org/10.1016/S0022-1694(01)00421-8.

Beven, K.J., 2009. Environmental Modelling: An Uncertain Future?: An Introduction to Techniques for Uncertainty Estimation in Environmental Prediction /Keith Beven. Routledge, London.

Blaurock, K., Beudert, B., Gilfedder, B.S., Fleckenstein, J.H., Peiffer, S., Hopp, L., 2021. Low hydrological connectivity after summer drought inhibits DOC export in a forested headwater catchment. Hydrol. Earth Syst. Sci. 25, 5133–5151. https://doi.org/10.5194/hess-25-5133-2021.

Boughton, W., 1989. A review of the USDA SCS curve number method. Soil Res. 27, 511–523.

Clark, J.M., Ashley, D., Wagner, M., Chapman, P.J., Lane, S.N., Evans, C.D., Heathwaite, A.L., 2009. Increased temperature sensitivity of net DOC production from ombrotrophic peat due to water table draw-down. Glob. Change Biol. 15, 794–807. https://doi.org/10.1111/j.1365-2486.2008.01683.x.

Clark, J.M., Bottrell, S.H., Evans, C.D., Monteith, D.T., Bartlett, R., Rose, R., Newton, R. J., Chapman, P.J., 2010. The importance of the relationship between scale and process in understanding long-term DOC dynamics. Sci. Total Environ. 408, 2768–2775. https://doi.org/10.1016/j.scitotenv.2010.02.046.

Cui, T., Sreekanth, J., Pickett, T., Rassam, D., Gilfedder, M., Barrett, D., 2021. Impact of model parameterization on predictive uncertainty of regional groundwater models in the context of environmental impact assessment. Environ. Impact Assess. Rev. 90, 106620. https://doi.org/10.1016/j.eiar.2021.106620.

de Wit, H.A., Mulder, J., Hindar, A., Hole, L., 2007. Long-term increase in dissolved organic carbon in streamwaters in Norway is response to reduced acid deposition. Environ. Sci. Technol. 41, 7706–7713. https://doi.org/10.1021/es070557f.

Diana, M., Felipe-Sotelo, M., Bond, T., 2019. Disinfection byproducts potentially responsible for the association between chlorinated drinking water and bladder cancer: a review. Water Res. 162, 492–504. https://doi.org/10.1016/j.watres.2019.07.014.

Dong, H., Zhang, S., Lin, J., Zhu, B., 2021. Responses of soil microbial biomass carbon and dissolved organic carbon to drying-rewetting cycles: a *meta*-analysis. CATENA 207, 105610. https://doi.org/10.1016/j.catena.2021.105610.

Doyle, B.C., de Eyto, E., Dillane, M., Poole, R., McCarthy, V., Ryder, E., Jennings, E., 2019. Synchrony in catchment stream colour levels is driven by both local and regional climate. Biogeosciences 16, 1053–1071. https://doi.org/10.5194/bg-16-1053-2019.

Doyle, B.C., de Eyto, E., McCarthy, V., Dillane, M., Poole, R., Jennings, E., 2021. Late summer peak in pCO_2 corresponds with catchment export of DOC in a temperate, humic lake. Inland Waters 11, 234–249. https://doi.org/10.1080/20442041.2021.1893098.

Du, J., Deng, G., 2022. How should a numerical weather prediction Be used: full field or anomaly? A conceptual demonstration with a Lorenz model. Atmosphere 13, 1487. https://doi.org/10.3390/atmos13091487.

Esper, J., Torbenson, M., Büntgen, U., 2024. 2023 summer warmth unparalleled over the past 2000 years. Nature 631, 94–97. https://doi.org/10.1038/s41586-024-07512-y.

Evans, C.D., Monteith, D.T., Cooper, D.M., 2005. Long-term increases in surface water dissolved organic carbon: observations, possible causes and environmental impacts. Environ. Pollut. 137, 55–71. https://doi.org/10.1016/j.envpol.2004.12.031. Recovery from acidificationin the UK: Evidence from 15 years of acid waters monitoring.

Evans, C.D., Chapman, P.J., Clark, J.M., Monteith, D.T., Cresser, M.S., 2006. Alternative explanations for rising dissolved organic carbon export from organic soils. Glob. Change Biol. 12, 2044–2053. https://doi.org/10.1111/j.1365-2486.2006.01241.x.

Fenner, N., Meadham, J., Jones, T., Hayes, F., Freeman, C., 2021. Effects of climate change on Peatland reservoirs: a DOC perspective. Glob. Biogeochem. Cycles 35. https://doi.org/10.1029/2021GB006992 e2021GB006992.

Franklin, H.M., Doederer, K., Neale, P.A., Hayton, J.B., Fisher, P., Maxwell, P., Carroll, A. R., Burford, M.A., Leusch, F.D.L., 2021. Terrestrial dissolved organic matter source affects disinfection by-product formation during water treatment and subsequent toxicity. Environ. Pollut. 283, 117232. https://doi.org/10.1016/j.envpol.2021.117232.

Futter, M.N., Löfgren, S., Köhler, S.J., Lundin, L., Moldan, F., Bringmark, L., 2011. Simulating dissolved organic carbon dynamics at the Swedish Integrated Monitoring sites with the integrated catchments model for carbon, INCA-C. Ambio 40, 906–919. https://doi.org/10.1007/s13280-011-0203-z.

Garmo, Ø.A., Skjelkvåle, B.L., de Wit, H.A., Colombo, L., Curtis, C., Fölster, J., Hoffmann, A., Hruška, J., Høgåsen, T., Jeffries, D.S., Keller, W.B., Krám, P., Majer, V., Monteith, D.T., Paterson, A.M., Rogora, M., Rzychon, D., Steingruber, S., Stoddard, J.L., Vuorenmaa, J., Worsztynowicz, A., 2014. Trends in surface water chemistry in acidified areas in Europe and North America from 1990 to 2008. Water, Air, Soil Pollut. 225, 1880. https://doi.org/10.1007/s11270-014-1880-6.

Haith, D.A., Shoemaker, L.L., 1987. Generalized watershed loading functions for stream flow Nutrients1. JAWRA J. Am. Water Resour. Assoc. 23, 471–478. https://doi.org/10.1111/j.1752-1688.1987.tb00825.x.

Hamon, W.R., 1961. Estimating potential evapotranspiration. J. Hydraul. Div. 87, 107–120. https://doi.org/10.1061/JYCEAJ.0000599.

Hattermann, F.F., Vetter, T., Breuer, L., Su, B., Daggupati, P., Donnelly, C., Fekete, B., Flörke, F., Gosling, S.N., Hoffmann, P., Liersch, S., Masaki, Y., Motovilov, Y., Müller, C., Samaniego, L., Stacke, T., Wada, Y., Yang, T., Krysnaova, V., 2018. Sources of uncertainty in hydrological climate impact assessment: a cross-scale study. Environ. Res. Lett. 13, 015006. https://doi.org/10.1088/1748-9326/aa9938.

Her, Y., Yoo, S.-H., Cho, J., Hwang, S., Jeong, J., Seong, C., 2019a. Uncertainty in hydrological analysis of climate change: multi-parameter vs. multi-GCM ensemble predictions. Sci. Rep. 9, 4974. https://doi.org/10.1038/s41598-019-41334-7.

Her, Y., Yoo, S.-H., Cho, J., Hwang, S., Jeong, J., Seong, C., 2019b. Uncertainty in hydrological analysis of climate change: multi-parameter vs. multi-GCM ensemble predictions. Sci. Rep. 9, 4974. https://doi.org/10.1038/s41598-019-41334-7.

IPCC, Calvin, K., Dasgupta, D., Krinner, G., Mukherji, A., Thorne, P.W., Trisos, C., Romero, J., Aldunce, P., Barrett, K., Blanco, G., Cheung, W.W.L., Connors, S., Denton, F., Diongue-Niang, A., Dodman, D., Garschagen, M., Geden, O., Hayward, B., Jones, C., Jotzo, F., Krug, T., Lasco, R., Lee, Y.-Y., Masson-Delmotte, V., Meinshausen, M., Mintenbeck, K., Mokssit, A., Otto, F.E.L., Pathak, M., Pirani, A., Poloczanska, E., Pörtner, H.-O., Revi, A., Roberts, D.C., Roy, J., Ruane, A.C., Skea, J., Shukla, P.R., Slade, R., Slangen, A., Sokona, Y., Sörensson, A.A., Tignor, M., Van Vuuren, D., Wei, Y.-M., Winkler, H., Zhai, P., Zommers, Z., Hourcade, J.-C., Johnson, F.X., Pachauri, S., Simpson, N.P., Singh, C., Thomas, A., Totin, E., Arias, P., Bustamante, M., Elgizouli, I., Flato, G., Howden, M., Méndez-Vallejo, C., Pereira, J. J., Pichs-Madruga, R., Rose, S.K., Saheb, Y., Sánchez Rodríguez, R., Ürge-Vorsatz, D., Xiao, C., Yassaa, N., Alegría, A., Armour, K., Bednar-Friedl, B., Blok, K., Cissé, G., Dentener, F., Eriksen, S., Fischer, E., Garner, G., Guivarch, C., Haasnoot, M., Hansen, G., Hauser, M., Hawkins, E., Hermans, T., Kopp, R., Leprince-Ringuet, N., Lewis, J., Ley, D., Ludden, C., Niamir, L., Nicholls, Z., Some, S., Szopa, S., Trewin, B., Van Der Wijst, K.-I., Winter, G., Witting, M., Birt, A., Ha, M., Romero, J., Kim, J., Haites, E.F., Jung, Y., Stavins, R., Birt, A., Ha, M., Orendain, D.J.A., Ignon, L., Park, S., Park, Y., Reisinger, A., Cammaramo, D., Fischlin, A., Fuglestvedt, J.S., Hansen, G., Ludden, C., Masson-Delmotte, V., Matthews, J.B.R., Mintenbeck, K., Pirani, A., Poloczanska, E., Leprince-Ringuet, N., Péan, C., Core Writing Team, 2023. IPCC, 2023: climate change 2023: synthesis report. In: Lee, H., Romero, J. (Eds.), Contribution of Working Groups I, II and III to the Sixth Assessment Report of the Intergovernmental Panel on Climate Change. IPCC, Geneva, Switzerland. https://doi.org/10.59327/IPCC/AR6-9789291691647. Intergovernmental Panel on Climate Change (IPCC).

Jaafar, H.H., Ahmad, F.A., El Beyrouthy, N., 2019. GCN250, new global gridded curve numbers for hydrologic modeling and design. Sci. Data 6, 145. https://doi.org/10.1038/s41597-019-0155-x.

Jennings, E., Allott, N., Pierson, D.C., Schneiderman, E.M., Lenihan, D., Samuelsson, P., Taylor, D., 2009. Impacts of climate change on phosphorus loading from a grassland catchment: implications for future management. Water Res. 43, 4316–4326. https://doi.org/10.1016/j.watres.2009.06.032.

Jennings, E., Järvinen, M., Allott, N., Arvola, L., Moore, K., Naden, P., Aonghusa, C.N., Nõges, T., Weyhenmeyer, G.A., 2010. Impacts of climate on the flux of dissolved organic carbon from catchments. In: George, G. (Ed.), The Impact of Climate Change on European Lakes. Springer, Netherlands, Dordrecht, pp. 199–220. https://doi.org/10.1007/978-90-481-2945-4_12.

Jennings, E., de Eyto, E., Moore, T., Dillane, M., Ryder, E., Allott, N., Nic Aonghusa, C., Rouen, M., Poole, R., Pierson, D.C., 2020. From highs to lows: changes in dissolved organic carbon in a peatland catchment and lake following extreme flow events. Water 12. https://doi.org/10.3390/w12102843.

Johnes, P.J., Evershed, R.P., Jones, D.L., Maberly, S.C., 2023. Exploring the nature, origins and ecological significance of dissolved organic matter in freshwaters: state

of the science and new directions. Biogeochemistry 164, 1–12. https://doi.org/10.1007/s10533-023-01040-z.
Jutebring Sterte, E., Lidman, F., Sjöberg, Y., Ploum, S.W., Laudon, H., 2022. Groundwater travel times predict DOC in streams and riparian soils across a heterogeneous boreal landscape. Sci. Total Environ. 849, 157398. https://doi.org/10.1016/j.scitotenv.2022.157398.
Köhler, S.J., Lavonen, E., Keucken, A., Schmitt-Kopplin, P., Spanjer, T., Persson, K., 2016. Upgrading coagulation with hollow-fibre nanofiltration for improved organic matter removal during surface water treatment. Water Res. 89, 232–240. https://doi.org/10.1016/j.watres.2015.11.048.
Karhu, K., Fritze, H., Tuomi, M., Vanhala, P., Spetz, P., Kitunen, V., Liski, J., 2010. Temperature sensitivity of organic matter decomposition in two boreal forest soil profiles. Soil Biol. Biochem. 42, 72–82. https://doi.org/10.1016/j.soilbio.2009.10.002.
Klante, C., Hägg, K., Larson, M., 2022. Understanding short-term organic matter fluctuations to optimize drinking water treatment. Water Pract. Technol. 17, 2141–2159. https://doi.org/10.2166/wpt.2022.121.
Klimek, B., Chodak, M., Jaźwa, M., Azarbad, H., Niklińska, M., 2020. Soil physicochemical and microbial drivers of temperature sensitivity of soil organic matter decomposition under boreal forests. Pedosphere 30, 528–534. https://doi.org/10.1016/S1002-0160(17)60400-4.
Krause, P., Boyle, D.P., Bäse, F., 2005. Comparison of different efficiency criteria for hydrological model assessment. Adv. Geosci. 5, 89–97. https://doi.org/10.5194/adgeo-5-89-2005.
Kritzberg, E.S., Hasselquist, E.M., Škerlep, M., Löfgren, S., Olsson, O., Stadmark, J., Valinia, S., Hansson, L.-A., Laudon, H., 2020. Browning of freshwaters: consequences to ecosystem services, underlying drivers, and potential mitigation measures. Ambio 49, 375–390. https://doi.org/10.1007/s13280-019-01227-5.
Kumari, M., Gupta, S.K., 2022. Cumulative human health risk analysis of trihalomethanes exposure in drinking water systems. J. Environ. Manag. 321, 115949. https://doi.org/10.1016/j.jenvman.2022.115949.
Kundzewicz, Z.W., Krysanova, V., Benestad, R.E., Hov, Ø., Piniewski, M., Otto, I.M., 2018. Uncertainty in climate change impacts on water resources. Environ. Sci. Policy 79, 1–8. https://doi.org/10.1016/j.envsci.2017.10.008.
Lange, S., Büchner, M., 2021. ISIMIP3b bias-adjusted atmospheric climate input data (v1.1). https://doi.org/10.48364/ISIMIP.842396.1.
Ledesma, J.L.J., Köhler, S.J., Futter, M.N., 2012. Long-term dynamics of dissolved organic carbon: implications for drinking water supply. Sci. Total Environ. 432, 1–11. https://doi.org/10.1016/j.scitotenv.2012.05.071.
Lindqvist, K., 2022. Modelling the Effects of Climate Change on Future DOC Export to Lake Mälaren Using a Generalized Watershed Loading Functions (GWLF) Model. Uppsala University, Sweden.
Lofton, M.E., Brentrup, J.A., Beck, W.S., Zwart, J.A., Bhattacharya, R., Brighenti, L.S., Burnet, S.H., McCullough, I.M., Steele, B.G., Carey, C.C., Cottingham, K.L., Dietze, M.C., Ewing, H.A., Weathers, K.C., LaDeau, S.L., 2022. Using near-term forecasts and uncertainty partitioning to inform prediction of oligotrophic lake cyanobacterial density. Ecol. Appl. 32, e2590. https://doi.org/10.1002/eap.2590.
Marshall, A.M., Link, T.E., Flerchinger, G.N., Lucash, M.S., 2021. Importance of parameter and climate data uncertainty for future changes in boreal hydrology. Water Resour. Res. 57. https://doi.org/10.1029/2021WR029911 e2021WR029911.
Mozafari, B., Bruen, M., Donohue, S., Renou-Wilson, F., O'Loughlin, F., 2023. Peatland dynamics: a review of process-based models and approaches. Sci. Total Environ. 877, 162890. https://doi.org/10.1016/j.scitotenv.2023.162890.
Naden, P.S., Allott, N., Arvola, L., Järvinen, M., Jennings, E., Moore, K., Nic Aonghusa, C., Pierson, D., Schneiderman, E., 2010. Modelling the impacts of climate change on dissolved organic carbon. In: George, G. (Ed.), The Impact of Climate Change on European Lakes. Springer, Netherlands, Dordrecht, pp. 221–252. https://doi.org/10.1007/978-90-481-2945-4_13.
O'Driscoll, C., Ledesma, J.L.J., Coll, J., Murnane, J.G., Nolan, P., Mockler, E.M., Futter, M.N., Xiao, L.W., 2018a. Minimal climate change impacts on natural organic matter forecasted for a potable water supply in Ireland. Sci. Total Environ. 630, 869–877. https://doi.org/10.1016/j.scitotenv.2018.02.248.
O'Driscoll, C., Sheahan, J., Renou-Wilson, F., Croot, P., Pilla, F., Misstear, B., Xiao, L., 2018b. National scale assessment of total trihalomethanes in Irish drinking water. J. Environ. Manag. 212, 131–141. https://doi.org/10.1016/j.jenvman.2018.01.070.
Oulehle, F., Hruška, J., 2009. Rising trends of dissolved organic matter in drinking-water reservoirs as a result of recovery from acidification in the Ore Mts., Czech Republic. Environ. Pollut. 157, 3433–3439. https://doi.org/10.1016/j.envpol.2009.06.020. Persistent Organic Pollutants in Mountainous Areas.
Piai, L., Mei, S., van Gijn, K., Langenhoff, A., 2024. Effects of organic matter in drinking water and wastewater on micropollutant adsorption to activated carbon. Int. J. Environ. Sci. Technol. 21, 2547–2558. https://doi.org/10.1007/s13762-023-05132-z.
Pianosi, F., Beven, K., Freer, J., Hall, J.W., Rougier, J., Stephenson, D.B., Wagener, T., 2016. Sensitivity analysis of environmental models: a systematic review with practical workflow. Environ. Model. Softw. 79, 214–232. https://doi.org/10.1016/j.envsoft.2016.02.008.
Ploum, S., Laudon, H., Peralta Tapia, A., Kuglerová, L., 2020. Are dissolved organic carbon concentrations in riparian groundwater linked to hydrological pathways in the boreal forest? Hydrol. Earth Syst. Sci. 24, 1709–1720. https://doi.org/10.5194/hess-24-1709-2020.
Prijac, A., Gandois, L., Taillardat, P., Bourgault, M.-A., Riahi, K., Ponçot, A., Tremblay, A., Garneau, M., 2023. Hydrological connectivity controls dissolved organic carbon exports in a peatland-dominated boreal catchment stream. Hydrol. Earth Syst. Sci. 27, 3935–3955. https://doi.org/10.5194/hess-27-3935-2023.
Ripple, W.J., Wolf, C., Gregg, J.W., Rockström, J., Newsome, T.M., Law, B.E., Marques, L., Lenton, T.M., Xu, C., Huq, S., Simons, L., King, S.D.A., 2023. The 2023 state of the climate report: entering uncharted territory. Bioscience 73, 841–850. https://doi.org/10.1093/biosci/biad080.
Ritson, J.P., Graham, N.J.D., Templeton, M.R., Clark, J.M., Gough, R., Freeman, C., 2014. The impact of climate change on the treatability of dissolved organic matter (DOM) in upland water supplies: a UK perspective. Sci. Total Environ. 473-474, 714–730. https://doi.org/10.1016/j.scitotenv.2013.12.095.
Riyadh, A., Peleato, N.M., 2024. Natural organic matter character in drinking water distribution systems: a review of impacts on water quality and characterization techniques. Water 16, 446. https://doi.org/10.3390/w16030446.
Rodríguez-Cardona, B.M., Wymore, A.S., Argerich, A., Barnes, R.T., Bernal, S., Brookshire, E.N.J., Coble, A.A., Dodds, W.K., Fazekas, H.M., Helton, A.M., Johnes, P. J., Johnson, S.L., Jones, J.B., Kaushal, S.S., Kortelainen, P., López-Lloreda, C., Spencer, R.G.M., McDowell, W.H., 2022. Shifting stoichiometry: long-term trends in stream-dissolved organic matter reveal altered C:N ratios due to history of atmospheric acid deposition. Glob. Change Biol. 28, 98–114. https://doi.org/10.1111/gcb.15965.
Ryder, E., de Eyto, E., Dillane, M., Poole, R., Jennings, E., 2014. Identifying the role of environmental drivers in organic carbon export from a forested peat catchment. Sci. Total Environ. 490, 28–36. https://doi.org/10.1016/j.scitotenv.2014.04.091.
SanClements, M.D., Oelsner, G.P., McKnight, D.M., Stoddard, J.L., Nelson, S.J., 2012. New insights into the source of decadal increases of dissolved organic matter in acid-sensitive lakes of the northeastern United States. Environ. Sci. Technol. 46, 3212–3219. https://doi.org/10.1021/es204321x.
Schürz, C., Hollosi, B., Matulla, C., Pressl, A., Ertl, T., Schulz, K., Mehdi, B., 2019. A comprehensive sensitivity and uncertainty analysis for discharge and nitrate-nitrogen loads involving multiple discrete model inputs under future changing conditions. Hydrol. Earth Syst. Sci. 23, 1211–1244. https://doi.org/10.5194/hess-23-1211-2019.
Schneiderman, E.M., Pierson, D.C., Lounsbury, D.G., Zion, M.S., 2002. Modeling of hydrochemistry of the cannonsville watershed with Generalized Watershed loading functions (GWLF). JAWRA J. Am. Water Resour. Assoc. 38, 1323–1347. https://doi.org/10.1111/j.1752-1688.2002.tb04350.x.
Schneiderman, E., Järvinen, M., Jennings, E., May, L., Moore, K., Naden, P.S., Pierson, D., 2010. Modeling the effects of climate change on catchment hydrology with the GWLF model. In: George, G. (Ed.), The Impact of Climate Change on European Lakes. Springer, Netherlands, Dordrecht, pp. 33–50. https://doi.org/10.1007/978-90-481-2945-4_3.
Son, K., Lin, L., Band, L., Owens, E.M., 2019. Modelling the interaction of climate, forest ecosystem, and hydrology to estimate catchment dissolved organic carbon export. Hydrol. Process. 33, 1448–1464. https://doi.org/10.1002/hyp.13412.
Srivastav, A.L., Patel, N., Chaudhary, V.K., 2020. Disinfection by-products in drinking water: occurrence, toxicity and abatement. Environ. Pollut. 267, 115474. https://doi.org/10.1016/j.envpol.2020.115474.
Teweldebrhan, A.T., Burkhart, J.F., Schuler, T.V., 2018. Parameter uncertainty analysis for an operational hydrological model using residual-based and limits of acceptability approaches. Hydrol. Earth Syst. Sci. 22, 5021–5039. https://doi.org/10.5194/hess-22-5021-2018.
van der Wiel, K., Bintanja, R., 2021. Contribution of climatic changes in mean and variability to monthly temperature and precipitation extremes. Commun. Earth Environ. 2, 1–11. https://doi.org/10.1038/s43247-020-00077-4.
van Vliet, M.T.H., Thorslund, J., Strokal, M., Hofstra, N., Flörke, M., Ehalt Macedo, H., Nkwasa, A., Tang, T., Kaushal, S.S., Kumar, R., van Griensven, A., Bouwman, L., Mosley, L.M., 2023. Global river water quality under climate change and hydroclimatic extremes. Nat. Rev. Earth Environ. 4, 687–702. https://doi.org/10.1038/s43017-023-00472-3.
Villanueva, C.M., Evlampidou, I., Ibrahim, F., Donat-Vargas, C., Valentin, A., Tugulea, A.-M., Echigo, S., Jovanovic, D., Lebedev, A.T., Lemus-Pérez, M., Rodriguez-Susa, M., Luzati, A., de Cássia dos Santos Nery, T., Pastén, P.A., Quiñones, M., Regli, S., Weisman, R., Dong, S., Ha, M., Phattarapattamawong, S., Manasfi, T., Musah, S.-I.E., Eng, A., Janák, K., Rush, S.C., Reckhow, D., Krasner, S. W., Vineis, P., Richardson, S.D., Kogevinas, M., 2023. Global assessment of chemical quality of drinking water: the case of trihalomethanes. Water Res. 230, 119568. https://doi.org/10.1016/j.watres.2023.119568.
Wang, X., Jiang, D., Lang, X., 2017. Future extreme climate changes linked to global warming intensity. Sci. Bull. 62, 1673–1680. https://doi.org/10.1016/j.scib.2017.11.004.
Warner, K.A., Saros, J.E., 2019. Variable responses of dissolved organic carbon to precipitation events in boreal drinking water lakes. Water Res. 156, 315–326. https://doi.org/10.1016/j.watres.2019.03.036.
Watling, J.I., Brandt, L.A., Bucklin, D.N., Fujisaki, I., Mazzotti, F.J., Romañach, S.S., Speroterra, C., 2015. Performance metrics and variance partitioning reveal sources of uncertainty in species distribution models. Ecol. Model. 309-310, 48–59. https://doi.org/10.1016/j.ecolmodel.2015.03.017.
Wei, X., Hayes, D.J., Butman, D.E., Qi, J., Ricciuto, D.M., Yang, X., 2024. Modeling exports of dissolved organic carbon from landscapes: a review of challenges and opportunities. Environ. Res. Lett. 19, 053001. https://doi.org/10.1088/1748-9326/ad3cf8.
Williamson, J., Evans, C., Spears, B., Pickard, A., Chapman, P.J., Feuchtmayr, H., Leith, F., Waldron, S., Monteith, D., 2023. Reviews and syntheses: understanding the impacts of peatland catchment management on dissolved organic matter concentration and treatability. Biogeosciences 20, 3751–3766. https://doi.org/10.5194/bg-20-3751-2023.
Wit, H.A.de, Stoddard, J.L., Monteith, D.T., Sample, J.E., Austnes, K., Couture, S., Fölster, J., Higgins, S.N., Houle, D., Hruška, J., Krám, P., Kopáček, J., Paterson, A.M.,

Valinia, S., Dam, H.V., Vuorenmaa, J., Evans, C.D., 2021. Cleaner air reveals growing influence of climate on dissolved organic carbon trends in northern headwaters. Environ. Res. Lett. 16, 104009. https://doi.org/10.1088/1748-9326/ac2526.

Wu, J., Yao, H., 2022. Simulating dissolved organic carbon during dryness/wetness periods based on hydrological characteristics under multiple timescales. J. Hydrol. 614, 128534. https://doi.org/10.1016/j.jhydrol.2022.128534.

Wu, J., Yao, H., 2024. Enhanced role of streamflow processes in the evolutionary trends of dissolved organic carbon. Environ. Sci. Technol. 58, 4772–4780. https://doi.org/10.1021/acs.est.3c09508.

Wu, J., Yao, H., Chen, X., Chen, X., 2023a. Dynamics of dissolved organic carbon during drought and flood events: a phase-by-stages perspective. Sci. Total Environ. 871, 162158. https://doi.org/10.1016/j.scitotenv.2023.162158.

Wu, J., Yao, H., Wang, G., Chen, X., Yuan, X., Zhou, Y., Zhang, D., 2023b. Dynamics of DOC concentration and flux in different propagation stages of hydrological drought: patterns and drivers. J. Hydrol. 617, 128939. https://doi.org/10.1016/j.jhydrol.2022.128939.

Xiao, R., Deng, Y., Xu, Z., Chu, W., 2024. Disinfection byproducts and their precursors in drinking water sources: origins, influencing factors, and environmental insights. Engineering 36, 36–50. https://doi.org/10.1016/j.eng.2023.08.017.

Xu, J., Morris, P.J., Liu, J., Holden, J., 2018. Hotspots of peatland-derived potable water use identified by global analysis. Nat. Sustain. 1, 246–253. https://doi.org/10.1038/s41893-018-0064-6.

Xu, J., Morris, P.J., Liu, J., Ledesma, J.L.J., Holden, J., 2020. Increased dissolved organic carbon concentrations in peat-fed UK water supplies under future climate and sulfate deposition scenarios. Water Resour. Res. 56. https://doi.org/10.1029/2019WR025592 e2019WR025592.

Zhong, J., Cai, W., 2015. Differential evolution with sensitivity analysis and the Powell's method for crowd model calibration. J. Comput. Sci., Comput. Sci. Gates Nat. 9, 26–32. https://doi.org/10.1016/j.jocs.2015.04.013.